

Mesonic Form Factors and the Isgur-Wise Function on the Light-Front

Hai-Yang Cheng^a, Chi-Yee Cheung^a, Chien-Wen Hwang^{a,b}

^a*Institute of Physics, Academia Sinica, Taipei, Taiwan 115, Republic of China*

^b*Department of Physics, National Taiwan University, Taipei, Taiwan 107, Republic of China*
(July, 1996)

Abstract

Within the light-front framework, form factors for $P \rightarrow P$ and $P \rightarrow V$ transitions (P : pseudoscalar meson, V : vector meson) due to the valence-quark configuration are calculated directly in the entire physical range of momentum transfer. The behavior of the form factors in the infinite quark mass limit are examined to see if the requirements of heavy-quark symmetry are fulfilled. We find that the Bauer-Stech-Wirbel type of light-front wave function fails to give a correct normalization for the Isgur-Wise function at zero recoil in $P \rightarrow V$ transition. Some of the $P \rightarrow V$ form factors are found to depend on the recoiling direction of the daughter mesons relative to their parents. Thus, the inclusion of the non-valence contribution arising from quark-pair creation is mandatory in order to ensure that the physical form factors are independent of the recoiling direction. The main feature of the non-valence contribution is discussed.

PACS numbers: 13.20, 14.40.J

I. INTRODUCTION

The hadronic matrix element of weak $P \rightarrow P$ transition (P : pseudoscalar meson) is described by two form factors, whereas in general it requires four form factors to parametrize the weak matrix element for $P \rightarrow V$ transition (V : vector meson). Heavy quark symmetry predicts that, all the mesonic form factors in the infinite quark mass limit $m_Q \rightarrow \infty$ are related to a single universal Isgur-Wise function [1]. The symmetry breaking $1/m_Q$ corrections can be studied in a systematic framework, namely the heavy quark effective theory (for a review, see [2]). The Isgur-Wise function is normalized to unity at zero recoil, but otherwise remains unknown. Phenomenologically, the hadronic form factors can be evaluated in various models among which the quark model is a popular one. However, since usual quark-model wave functions best resemble meson states in the rest frame or where the meson velocities are small, hence the form factors calculated in non-relativistic quark model or the MIT bag model are trustworthy only when the recoil momentum of the daughter meson relative to the parent meson is small.

As the recoil momentum increases (corresponding to a decreasing q^2), we have to start considering relativistic effects seriously. In particular, at the maximum recoil point $q^2 = 0$ where the final meson could be highly relativistic, there is no reason to expect that the non-relativistic quark model is still applicable. A consistent treatment of the relativistic effects of the quark motion and spin in a bound state is a main issue of the relativistic quark model. To our knowledge, the light-front quark model [3,4] is the only relativistic quark model in which a consistent and fully relativistic treatment of quark spins and the center-of-mass motion can be carried out. This model has many advantages. For example, the light-front wave function is manifestly Lorentz invariant as it is expressed in terms of the momentum fraction variables (in “+” components) in analog to the parton distributions in the infinite momentum frame. Moreover, hadron spin can also be correctly constructed using the so-called Melosh rotation. The kinematic subgroup of the light-front formalism has the maximum number of interaction-free generators including the boost operator which describes the center-of-mass motion of the bound state (for a review of the light-front dynamics and light-front QCD, see [5]).

The light-front quark model has been applied in the past to study the heavy-to-heavy

and heavy-to-light weak decays form factors [6–9]. However, the weak form factors were calculated only for $q^2 \leq 0$, whereas physical decays occur in the time-like region $0 \leq q^2 \leq (M_i - M_f)^2$, with $M_{i,f}$ being the initial and final meson masses. Hence extra assumptions are needed to extrapolate the form factors to cover the entire range of momentum transfer. In [10] an ansatz for the q^2 dependence was made to extrapolate the form factors in the space-like region to the time-like region. Based on the dispersion formulation, form factors at $q^2 > 0$ were obtained in [11] by performing an analytic continuation from the space-like q^2 region. Finally, the weak form factors for $P \rightarrow P$ transition were calculated in [12–14] for the first time for the entire range of q^2 , so that additional extrapolation assumptions are no longer required. This is based on the observation [15] that in the frame where the momentum transfer is purely longitudinal, i.e., $q_\perp = 0$, $q^2 = q^+ q^-$ covers the entire range of momentum transfer. The price one has to pay is that, besides the conventional valence-quark contribution, one must also consider the non-valence configuration (or the so-called Z -graph) arising from quark-pair creation from the vacuum (see Fig. 1). The non-valence contribution vanishes if $q^+ = 0$, but is supposed to be important for heavy-to-light transition near zero recoil [6,10,15,16]. Unfortunately, a reliable way of estimating the Z -graph contribution is still lacking.

In the present paper we calculate the $P \rightarrow V$ form factors directly at time-like momentum transfers for the first time. We then study the mesonic form factors in the infinite quark mass limit to check if the light-front model calculations respect heavy quark symmetry. We are able to compute the Isgur-Wise function exactly since the non-valence contribution vanishes in the heavy-quark limit. It turns out that not all light-front wave functions give a correct normalization for the Isgur-Wise function at zero recoil in $P \rightarrow V$ decay. In other words, the requirement of heavy quark symmetry can be utilized to rule out certain phenomenological wave functions.

Another issue we would like to address in this work has to do with reference frame dependence of form factor. For a given q^2 , one can choose whether the recoiling daughter meson moves in the positive or negative z -direction relative to the parent meson, which we call the “+” and “−” reference frame, respectively. For some form factors in $P \rightarrow V$ transition, namely A_0 , A_1 , V , valence-quark and non-valence contributions are separately dependent on the choice of the “+” or “−” frame, but their sum should not. This demonstrates the

fact that it is mandatory to take into account the non-valence configuration in order to have physical predictions for form factors. This issue will be discussed in more details in Sections IID and IVC.

This paper is organized as follows. In Section II, the basic theoretical formalism is given and form factors for $P \rightarrow P$ and $P \rightarrow V$ transitions are derived. Section III is devoted to the discussion of the Isgur-Wise function. Numerical results are present and discussed in Section IV, and finally a summary is given in Section V.

II. FRAMEWORK

We will describe in this section the light-front approach for the calculation of the weak mesonic form factors for pseudoscalar-to-pseudoscalar and pseudoscalar-to-vector transitions. The hadronic matrix elements will be evaluated at time-like momentum transfers, namely the physically accessible kinematic region $0 \leq q^2 \leq q_{\text{max}}^2$.

A meson bound state consisting of a quark q_1 and an antiquark \bar{q}_2 with total momentum P and spin S can be written as

$$|M(P, S, S_z)\rangle = \int \{d^3p_1\} \{d^3p_2\} 2(2\pi)^3 \delta^3(\tilde{P} - \tilde{p}_1 - \tilde{p}_2) \times \sum_{\lambda_1, \lambda_2} \Psi^{SS_z}(\tilde{p}_1, \tilde{p}_2, \lambda_1, \lambda_2) |q_1(p_1, \lambda_1) \bar{q}_2(p_2, \lambda_2)\rangle, \quad (2.1)$$

where p_1 and p_2 are the on-mass-shell light-front momenta,

$$\tilde{p} = (p^+, p_\perp), \quad p_\perp = (p^1, p^2), \quad p^- = \frac{m^2 + p_\perp^2}{p^+}, \quad (2.2)$$

and

$$\begin{aligned} \{d^3p\} &\equiv \frac{dp^+ d^2p_\perp}{2(2\pi)^3}, \\ |q(p_1, \lambda_1) \bar{q}(p_2, \lambda_2)\rangle &= b_{\lambda_1}^\dagger(p_1) d_{\lambda_2}^\dagger(p_2) |0\rangle, \\ \{b_{\lambda'}(p'), b_\lambda^\dagger(p)\} &= \{d_{\lambda'}(p'), d_\lambda^\dagger(p)\} = 2(2\pi)^3 \delta^3(\tilde{p}' - \tilde{p}) \delta_{\lambda'\lambda}. \end{aligned} \quad (2.3)$$

In terms of the light-front relative momentum variables (x, k_\perp) defined by

$$\begin{aligned} p_1^+ &= x_1 P^+, \quad p_2^+ = x_2 P^+, \quad x_1 + x_2 = 1, \\ p_{1\perp} &= x_1 P_\perp + k_\perp, \quad p_{2\perp} = x_2 P_\perp - k_\perp, \end{aligned} \quad (2.4)$$

the momentum-space wave-function Ψ^{SS_z} can be expressed as

$$\Psi^{SS_z}(\tilde{p}_1, \tilde{p}_2, \lambda_1, \lambda_2) = R_{\lambda_1 \lambda_2}^{SS_z}(x, k_\perp) \phi(x, k_\perp), \quad (2.5)$$

where $\phi(x, k_\perp)$ describes the momentum distribution of the constituents in the bound state, and $R_{\lambda_1 \lambda_2}^{SS_z}$ constructs a state of definite spin (S, S_z) out of light-front helicity (λ_1, λ_2) eigenstates. Explicitly,

$$R_{\lambda_1 \lambda_2}^{SS_z}(x, k_\perp) = \sum_{s_1, s_2} \langle \lambda_1 | \mathcal{R}_M^\dagger(1-x, k_\perp, m_1) | s_1 \rangle \langle \lambda_2 | \mathcal{R}_M^\dagger(x, -k_\perp, m_2) | s_2 \rangle \langle \frac{1}{2} s_1 \frac{1}{2} s_2 | S S_z \rangle, \quad (2.6)$$

where $|s_i\rangle$ are the usual Pauli spinor, and \mathcal{R}_M is the Melosh transformation operator:

$$\mathcal{R}_M(x, k_\perp, m_i) = \frac{m_i + x_i M_0 + i \vec{\sigma} \cdot \vec{k}_\perp \times \vec{n}}{\sqrt{(m_i + x_i M_0)^2 + k_\perp^2}}, \quad (2.7)$$

with $\vec{n} = (0, 0, 1)$, a unit vector in the z -direction, and

$$M_0^2 = \frac{m_1^2 + k_\perp^2}{x_1} + \frac{m_2^2 + k_\perp^2}{x_2}. \quad (2.8)$$

In practice it is more convenient to use the covariant form for $R_{\lambda_1 \lambda_2}^{SS_z}$ [6]:

$$R_{\lambda_1 \lambda_2}^{SS_z}(x, k_\perp) = \frac{\sqrt{p_1^+ p_2^+}}{\sqrt{2} \widetilde{M}_0} \bar{u}(p_1, \lambda_1) \Gamma v(p_2, \lambda_2), \quad (2.9)$$

where

$$\begin{aligned} \widetilde{M}_0 &\equiv \sqrt{M_0^2 - (m_1 - m_2)^2}, \\ \Gamma &= \gamma_5 \quad (\text{pseudoscalar}, S=0), \\ \Gamma &= - \not{\varepsilon}(S_z) + \frac{\hat{\varepsilon} \cdot (p_1 - p_2)}{M_0 + m_1 + m_2} \quad (\text{vector}, S=1), \end{aligned} \quad (2.10)$$

with

$$\begin{aligned} \hat{\varepsilon}^\mu(\pm 1) &= \left[\frac{2}{P^+} \vec{\varepsilon}_\perp(\pm 1) \cdot \vec{P}_\perp, 0, \vec{\varepsilon}_\perp(\pm 1) \right], \quad \vec{\varepsilon}_\perp(\pm 1) = \mp(1, \pm i)/\sqrt{2}, \\ \hat{\varepsilon}^\mu(0) &= \frac{1}{M_0} \left(\frac{-M_0^2 + P_\perp^2}{P^+}, P^+, P_\perp \right). \end{aligned} \quad (2.11)$$

Note that the longitudinal polarization 4-vector $\hat{\varepsilon}^\mu(0)$ given above is not exactly the same as that of the vector meson [cf. Eq.(2.47)]. We normalize the meson state as

$$\langle M(P', S', S'_z) | M(P, S, S_z) \rangle = 2(2\pi)^3 P^+ \delta^3(\tilde{P}' - \tilde{P}) \delta_{S'S} \delta_{S'_z S_z}, \quad (2.12)$$

so that

$$\int \frac{dx d^2 k_\perp}{2(2\pi)^3} |\phi(x, k_\perp)|^2 = 1. \quad (2.13)$$

In principle, the momentum distribution amplitude $\phi(x, k_\perp)$ can be obtained by solving the light-front QCD bound state equation [5,17]. However, before such first-principles solutions are available, we would have to be contented with phenomenological amplitudes. One example that has been often used in the literature for heavy mesons is the so-called Bauer-Stech-Wirbel (BSW) amplitude [18], which for a meson of mass M is given by

$$\phi(x, k_\perp)_{\text{BSW}} = \mathcal{N} \sqrt{x(1-x)} \exp\left(\frac{-k_\perp^2}{2\omega^2}\right) \exp\left[-\frac{M^2}{2\omega^2}(x-x_0)^2\right], \quad (2.14)$$

where \mathcal{N} is a normalization constant, x is the longitudinal momentum fraction carried by the light antiquark, $x_0 = (\frac{1}{2} - \frac{m_1^2 - m_2^2}{2M^2})$, and ω is a parameter of order Λ_{QCD} .

An other example is the Gaussian-type wave function,

$$\phi(x, k_\perp)_{\text{Gauss}} = \mathcal{N} \sqrt{\frac{dk_z}{dx}} \exp\left(-\frac{\vec{k}^2}{2\omega^2}\right), \quad (2.15)$$

where $\mathcal{N} = 4(\pi/\omega^2)^{3/4}$, and k_z of the internal momentum $\vec{k} = (\vec{k}_\perp, k_z)$ is defined through

$$x = \frac{e_1 - k_z}{e_1 + e_2}, \quad 1 - x = \frac{e_2 + k_z}{e_1 + e_2}, \quad (2.16)$$

with $e_i = \sqrt{m_i^2 + \vec{k}^2}$. We then have

$$M_0 = e_1 + e_2, \quad k_z = \frac{xM_0}{2} - \frac{m_2^2 + k_\perp^2}{2xM_0}, \quad (2.17)$$

and

$$\frac{dk_z}{dx} = \frac{e_1 e_2}{x(1-x)M_0} \quad (2.18)$$

is the Jacobian of transformation from (x, k_\perp) to \vec{k} . This wave function has been also used in many other studies of hadronic transitions. In particular, with appropriate parameters, it describes satisfactorily the pion elastic form factor up to $Q^2 \sim 10 \text{ GeV}^2$ [4]. A variant of the Gaussian-type wave function is

$$\phi(x, k_\perp) = \mathcal{N} \sqrt{\frac{dk_z}{dx}} \exp\left(-\frac{M_0^2}{2\omega^2}\right), \quad (2.19)$$

with M_0 being given by (2.8). This amplitude is equivalent to $\phi(x, k_\perp)_{\text{Gauss}}$ when the constituent quark masses are equal but becomes different otherwise. Nevertheless, we will not pursue this wave function further because it does not have an appropriate heavy-quark-limit behavior (see Sec. III).

Obviously, the Isgur-Wise function for heavy meson transitions depends on the heavy meson wave function $\phi(x, k_\perp)$ chosen. It turns out that in contrast to the Gaussian-type wave function, the BSW wave function fails to give a correct normalization for the Isgur-Wise function at zero recoil in $P \rightarrow V$ transition.

A. Decay Constants

The decay constant of a pseudoscalar meson $P(q_1 \bar{q}_2)$ defined by $\langle 0 | A^\mu | P \rangle = i f_P p^\mu$ can be evaluated using the light-front wave function given by (2.1) and (2.5)

$$\begin{aligned} \langle 0 | \bar{q}_2 \gamma^+ \gamma_5 q_1 | P \rangle &= \int \{d^3 p_1\} \{d^3 p_2\} 2(2\pi)^3 \delta(P - p_1 - p_2) \phi_P(x, k_\perp) R_{\lambda_1 \lambda_2}^{00}(x, k_\perp) \\ &\times \langle 0 | \bar{q}_2 \gamma^+ \gamma_5 q_1 | q_1 \bar{q}_2 \rangle. \end{aligned} \quad (2.20)$$

Since $\widetilde{M}_0 \sqrt{x(1-x)} = \sqrt{\mathcal{A}^2 + k_\perp^2}$, it is straightforward to show that

$$f_P = 4 \frac{\sqrt{3}}{\sqrt{2}} \int \frac{dx d^2 k_\perp}{2(2\pi)^3} \phi_P(x, k_\perp) \frac{\mathcal{A}}{\sqrt{\mathcal{A}^2 + k_\perp^2}}, \quad (2.21)$$

where

$$\mathcal{A} = m_1 x + m_2 (1 - x). \quad (2.22)$$

Note that the factor $\sqrt{3}$ in (2.21) arises from the color factor implicit in the meson wave function.

Likewise, for the vector-meson decay constant defined by

$$\langle 0 | V^\mu | V \rangle = f_V M_V \varepsilon^\mu, \quad (2.23)$$

is found to be

$$\begin{aligned} f_V &= 4 \frac{\sqrt{3}}{\sqrt{2}} \int \frac{dx d^2 k_\perp}{2(2\pi)^3} \frac{\phi_V(x, k_\perp)}{\sqrt{\mathcal{A}^2 + k_\perp^2}} \frac{1}{M_V} \left\{ x(1-x) M_V^2 + m_1 m_2 + k_\perp^2 \right. \\ &\quad \left. + \frac{\mathcal{B}}{2m_V} \left[\frac{m_1^2 + k_\perp^2}{1-x} - \frac{m_2^2 + k_\perp^2}{x} - (1-2x) M_V^2 \right] \right\}, \end{aligned} \quad (2.24)$$

where

$$\mathcal{B} = xm_1 - (1-x)m_2, \quad W_V = M_0 + m_1 + m_2. \quad (2.25)$$

When the decay constant is known, it can be used to constrain the parameters of the light-front wave function.

B. Form Factors for $P \rightarrow P$ Transition

With the light-front wave functions given above, we will first calculate the form factors for $P \rightarrow P$ transitions given by

$$\langle P_2 | V^\mu | P_1 \rangle = f_+(q^2)(P_1 + P_2)^\mu + f_-(q^2)(P_1 - P_2)^\mu, \quad (2.26)$$

where $V^\mu = \bar{q}_2 \gamma^\mu q_1$. For later purposes, it is also convenient to parametrize this matrix element in different forms:

$$\begin{aligned} \langle P_2 | V^\mu | P_1 \rangle &= \sqrt{M_1 M_2} \left[h_+(q^2)(v_1 + v_2)^\mu + h_-(q^2)(v_1 - v_2)^\mu \right], \\ &= F_1(q^2) \left(P_1^\mu + P_2^\mu - \frac{M_1^2 - M_2^2}{q^2} q^\mu \right) + F_0(q^2) \frac{M_1^2 - M_2^2}{q^2} q^\mu, \end{aligned} \quad (2.27)$$

with $v_i \equiv P_i/M_i$, and

$$F_1(q^2) = f_+(q^2), \quad F_0(q^2) = f_+(q^2) + \frac{q^2}{M_1^2 - M_2^2} f_-(q^2). \quad (2.28)$$

In the heavy-quark limit $M_{1,2} \rightarrow \infty$, heavy-quark symmetry requires that [2]

$$h_+(q^2) = \xi(v_1 \cdot v_2), \quad h_-(q^2) = 0, \quad (2.29)$$

where $\xi(v_1 \cdot v_2)$ is the universal Isgur-Wise function normalized to unity at the point of equal velocities: $\xi(1) = 1$. The form factors F_1 and F_0 are related to the transition amplitude with the exchange of a vector (1^-) and a scalar (0^+) boson in the t -channel, respectively.

As explained in the Introduction, we shall work in the frame where $q_\perp = 0$ so that $q^2 = q^+ q^-$ will cover the whole time-like region $q^2 \geq 0$. Define $r \equiv P_2^+/P_1^+$ (it is denoted by R in [12]), then

$$q^2 = (1-r) \left(M_1^2 - \frac{M_2^2}{r} \right). \quad (2.30)$$

Consequently, for a given q^2 , there are two solutions for r :

$$r_{\pm} = \frac{M_2}{M_1} \left(v_1 \cdot v_2 \pm \sqrt{(v_1 \cdot v_2)^2 - 1} \right), \quad (2.31)$$

where $v_1 \cdot v_2$ is related to q^2 by

$$v_1 \cdot v_2 = \frac{M_1^2 + M_2^2 - q^2}{2M_1 M_2}. \quad (2.32)$$

The $+$ ($-$) signs in (2.31) correspond to the daughter meson recoiling in the positive (negative) z -direction relative to the parent meson (call them the “+” and “−” reference frame, respectively). At zero recoil ($q^2 = q_{\text{max}}^2$) and maximum recoil ($q^2 = 0$), r_{\pm} are given by

$$\begin{aligned} r_+(q_{\text{max}}^2) &= r_-(q_{\text{max}}^2) = \frac{M_2}{M_1}, \\ r_+(0) &= 1, \quad r_-(0) = \left(\frac{M_2}{M_1} \right)^2. \end{aligned} \quad (2.33)$$

The form factors $f_{\pm}(q^2)$ of course should be independent of the reference frame chosen for the moving direction of the daughter meson. For a given q^2 , suppose we obtain

$$\langle P_2 | V^+ | P_1 \rangle \Big|_{r=r_+} = 2P_1^+ H(r_+), \quad \langle P_2 | V^+ | P_1 \rangle \Big|_{r=r_-} = 2P_1^+ H(r_-). \quad (2.34)$$

It follows from (2.27) that

$$\begin{aligned} f_+(q^2) &= \frac{(1 - r_-)H(r_+) - (1 - r_+)H(r_-)}{r_+ - r_-}, \\ f_-(q^2) &= -\frac{(1 + r_-)H(r_+) - (1 + r_+)H(r_-)}{r_+ - r_-}. \end{aligned} \quad (2.35)$$

It is easily seen that $f_{\pm}(q^2)$ are independent of the choice of “+” or “−” frame, as it should be.

As noted earlier, in a frame with $q^+ > 0$, there are actually two distinct contributions to the hadronic matrix element [6,10,15,16]: valence (partonic) contribution calculated with relativistic light-front bound-state wave functions, and non-valence (non-partonic) contribution (or the so-called Z -graph) arising from quark-antiquark pair creation from the vacuum. In the following, we shall first provide some details for calculating the valence contribution, and then come back to the non-valence subprocess in Sec. II.D. For $P_1 = (q_1 \bar{q})$ and $P_2 = (q_2 \bar{q})$, the relevant quark momentum variables are

$$\begin{aligned}
p_1^+ &= (1-x)P_1^+, & p_{\bar{q}}^+ &= xP_1^+, & \vec{p}_{1\perp} &= (1-x)\vec{P}_{1\perp} + \vec{k}_\perp, & \vec{p}_{\bar{q}\perp} &= x\vec{P}_{1\perp} - \vec{k}_\perp, \\
p_2^+ &= (1-x')P_2^+, & p_{\bar{q}}'^+ &= x'P_2^+, & \vec{p}_{2\perp} &= (1-x')\vec{P}_{2\perp} + \vec{k}'_\perp, & \vec{p}_{\bar{q}\perp}' &= x'\vec{P}_{2\perp} - \vec{k}'_\perp,
\end{aligned} \tag{2.36}$$

where x (x') is the momentum fraction carried by the spectator antiquark \bar{q} in the initial (final) state. The spectator model requires that

$$p_{\bar{q}}'^+ = p_{\bar{q}}^+, \quad \vec{p}_{\bar{q}\perp}' = \vec{p}_{\bar{q}\perp}. \tag{2.37}$$

Taking a Lorentz frame where $\vec{P}_{1\perp} = \vec{P}_{2\perp} = 0$ amounts to having $\vec{q}_\perp = 0$ and $\vec{k}'_\perp = \vec{k}_\perp$. Then we readily obtain

$$\begin{aligned}
\langle P_2 | V^+ | P_1 \rangle &= \sum_{\lambda_1, \lambda_2, \bar{\lambda}} \int \{d^3 p_{\bar{q}}\} \phi_2^*(x', k_\perp) \phi_1(x, k_\perp) \\
&\quad \times R_{\lambda_2 \bar{\lambda}}^{00\dagger}(x', k_\perp) \bar{u}(p_2, \lambda_2) \gamma^+ u(p_1, \lambda_1) R_{\lambda_1 \bar{\lambda}}^{00}(x, k_\perp),
\end{aligned} \tag{2.38}$$

Substituting the covariant form given in Eq. (2.9) into Eq. (2.38) yields

$$\begin{aligned}
\langle P_2 | V^+ | P_1 \rangle &= \sqrt{\frac{1}{r}} \int \frac{dx d^2 k_\perp}{2(2\pi)^3} \phi_2^*(x', k_\perp) \phi_1(x, k_\perp) \frac{-1}{2\widetilde{M}_{02}\widetilde{M}_{01}\sqrt{(1-x')(1-x)}} \\
&\quad \times \text{Tr} \left[\gamma_5 (\not{p}_2 + m_2) \gamma^+ (\not{p}_1 + m_1) \gamma_5 (\not{p}_{\bar{q}} - m_{\bar{q}}) \right].
\end{aligned} \tag{2.39}$$

After some manipulation, the trace term in the above expression is reduced to

$$\text{Tr} \left[\gamma_5 (\not{p}_2 + m_2) \gamma^+ (\not{p}_1 + m_1) \gamma_5 (\not{p}_{\bar{q}} - m_{\bar{q}}) \right] = -\frac{4}{x'} (\mathcal{A}_1 \mathcal{A}_2 + k_\perp^2) P_1^+, \tag{2.40}$$

where

$$\mathcal{A}_1 = m_1 x + m_{\bar{q}}(1-x), \quad \mathcal{A}_2 = m_2 x' + m_{\bar{q}}(1-x'), \tag{2.41}$$

and use of (2.36) has been made. Since

$$\widetilde{M}_{01} \sqrt{x(1-x)} \widetilde{M}_{02} \sqrt{x'(1-x')} = \sqrt{\mathcal{A}_1^2 + k_\perp^2} \sqrt{\mathcal{A}_2^2 + k_\perp^2}, \tag{2.42}$$

we find from (2.34), (2.38), (2.40) and (2.42) that

$$H(r) = \int_0^r dx \int \frac{d^2 k_\perp}{2(2\pi)^3} \phi_2^*(x', k_\perp) \phi_1(x, k_\perp) \frac{\mathcal{A}_1 \mathcal{A}_2 + k_\perp^2}{\sqrt{\mathcal{A}_1^2 + k_\perp^2} \sqrt{\mathcal{A}_2^2 + k_\perp^2}}, \tag{2.43}$$

with $x' = x/r$. The form factors $f_\pm(q^2)$ can then be obtained from (2.35).

As stated before, in the literature these form factors are customarily evaluated in the frame where $q^+ = P_1^+ - P_2^+ = 0$. This leads to $q^2 = -q_\perp^2 \leq 0$, implying a space-like momentum transfer. The advantage of the condition $q^+ = 0$ is that form factors only receive valence contributions (see Sec. II.D). However, there are two drawbacks in this approach: First, form factors in the physical time-like region cannot be obtained without making additional q^2 extrapolation assumptions. Second, no information can be obtained for the form factor $f_-(q^2)$ since $P_2^+ = P_1^+$ [see (2.26)]. At the maximum recoil $q^2 = 0$, the form factor $f_+(0)$ is evaluated to be [6,9]

$$f_+(0) = \int_0^1 dx \int \frac{d^2 k_\perp}{2(2\pi)^3} \phi_2^*(x, k_\perp) \phi_1(x, k_\perp) \frac{\mathcal{A}_1 \mathcal{A}_2 + k_\perp^2}{\sqrt{\mathcal{A}_1^2 + k_\perp^2} \sqrt{\mathcal{A}_2^2 + k_\perp^2}}, \quad (2.44)$$

with \mathcal{A}_1 and \mathcal{A}_2 given by (2.41) except for that $x' = x$ here. Therefore, the results of (2.35) and (2.43) at $q^2 = 0$ are in agreement with (2.44).

C. Form Factors for $P \rightarrow V$ Transition

Form factors for $P \rightarrow V$ transition are defined as

$$\begin{aligned} \langle V(P_V, \varepsilon) | J_\mu | P(P_1) \rangle = & \frac{2}{M_P + M_V} i \epsilon_{\mu\nu\alpha\beta} \varepsilon^\nu P_V^\alpha P_1^\beta V(q^2) - \left[(M_P + M_V) \varepsilon_\mu A_1(q^2) \right. \\ & \left. - \frac{\varepsilon \cdot P_1}{M_P + M_V} (P_1 + P_V)_\mu A_2(q^2) - 2M_V \frac{\varepsilon \cdot P_1}{q^2} q_\mu (A_3(q^2) - A_0(q^2)) \right], \end{aligned} \quad (2.45)$$

where $J_\mu \equiv V_\mu - A_\mu$, $A_3(0) = A_0(0)$,

$$A_3(q^2) = \frac{M_P + M_V}{2M_V} A_1(q^2) - \frac{M_P - M_V}{2M_V} A_2(q^2), \quad (2.46)$$

and

$$\varepsilon^\mu(\pm 1) = \left(\frac{2\vec{\varepsilon}_\perp \cdot \vec{P}_{V\perp}}{P_V^+}, 0, \vec{\varepsilon}_\perp \right), \quad \varepsilon^\mu(0) = \frac{1}{M_V} \left(\frac{-M_V^2 + P_{V\perp}^2}{P_V^+}, P_V^+, \vec{P}_{V\perp} \right) \quad (2.47)$$

are, respectively, the transverse and longitudinal polarization vectors of the vector meson. The form factors A_1 and A_2 are related to 1^+ intermediate states, A_0 to 0^+ states, and V to 1^- states. The $P \rightarrow V$ matrix element can also be parametrized in different ways:

$$\begin{aligned} \langle V | J_\mu | P \rangle = & ig(q^2) \epsilon_{\mu\nu\alpha\beta} \varepsilon^\nu P_V^\alpha P_1^\beta + f(q^2) \varepsilon_\mu + (\varepsilon \cdot P_1) [a_+(q^2) (P_1 + P_V)_\mu + a_-(q^2) (P_1 - P_V)_\mu] \\ = & \sqrt{M_P M_V} \left\{ i \tilde{g}(q^2) \epsilon_{\mu\nu\alpha\beta} \varepsilon^\nu v'^\alpha v^\beta + \tilde{f}(q^2) \varepsilon_\mu \right. \\ & \left. + (\varepsilon \cdot v) [\tilde{a}_+(q^2) (v + v')_\mu + \tilde{a}_-(q^2) (v - v')_\mu] \right\}, \end{aligned} \quad (2.48)$$

where $v = P_1/M_P$ and $v' = P_V/M_V$. They are useful for later discussions. The form factors a_{\pm} , f and g are related to V , $A_{0,1,2,3}$ via

$$\begin{aligned} g(q^2) &= \frac{2}{M_P + M_V} V(q^2), \quad f(q^2) = -(M_P + M_V) A_1(q^2), \\ a_+(q^2) &= \frac{1}{M_P + M_V} A_2(q^2), \\ a_-(q^2) &= \frac{2M_V}{q^2} [A_3(q^2) - A_0(q^2)] \\ &= \frac{2M_V}{q^2} \left[\frac{M_P + M_V}{2M_V} A_1(q^2) - \frac{M_P - M_V}{2M_V} A_2(q^2) - A_0(q^2) \right]. \end{aligned} \quad (2.49)$$

Also,

$$\begin{aligned} \tilde{g}(q^2) &= \sqrt{M_P + M_V} g(q^2), \quad \tilde{f}(q^2) = \frac{f(q^2)}{\sqrt{M_P + M_V}}, \\ \tilde{a}_+(q^2) + \tilde{a}_-(q^2) &= \frac{M_P^2}{\sqrt{M_P M_V}} (a_+ + a_-), \quad \tilde{a}_+(q^2) - \tilde{a}_-(q^2) = \sqrt{M_P M_V} (a_+ - a_-). \end{aligned} \quad (2.50)$$

In the heavy-quark limit $M_P, M_V \rightarrow \infty$, heavy-quark symmetry demands that [2]

$$\tilde{a}_+ + \tilde{a}_- = 0, \quad \tilde{a}_+ - \tilde{a}_- = \tilde{g} = \xi(v \cdot v'), \quad \tilde{f} = -(1 + v \cdot v') \xi(v \cdot v'). \quad (2.51)$$

The calculation of the $P \rightarrow V$ form factors is more subtle than the $P \rightarrow P$ case. If we choose a frame where $P_{1\perp} = P_{V\perp} = 0$ as before, we will have $\varepsilon \cdot P_1 = 0$ for transverse polarization. As a result, form factors a_{\pm} in (2.48) cannot be separately determined. Therefore, we will let $P_{1\perp} = P_{V\perp} \neq 0$ at the outset, and set them to zero only after the form factors are extracted. With the transverse polarization $\varepsilon^\mu(\pm 1)$, form factors $a_{\pm}(q^2)$ and $g(q^2)$ can be individually determined. Then using the longitudinal polarization $\varepsilon^\mu(0)$, we are able to fix the remaining form factor $f(q^2)$.

We begin with $a_{\pm}(q^2)$. Since $\varepsilon^+(\pm 1) = 0$ [cf. (2.47)], it follows from (2.48) that

$$\begin{aligned} -\langle V(P_V) | A^+ | P(P_1) \rangle &= (\varepsilon \cdot P_1) [a_+(P_1^+ + P_V^+) + a_-(P_1^+ - P_V^+)] \\ &= \left(\frac{1}{r} - 1 \right) (\vec{\varepsilon}_\perp \cdot \vec{P}_\perp) [a_+(1 + r) + a_-(1 - r)] P_1^+, \end{aligned} \quad (2.52)$$

with $r \equiv P_V^+/P_1^+$ and $P_\perp \equiv P_{1\perp} = P_{V\perp}$. As will be shown below, the above matrix element at the quark level has the form

$$\langle V | A^+ | P \rangle = 2\vec{\varepsilon}_\perp \cdot \vec{P}_\perp (1 - r) I(r) P_1^+. \quad (2.53)$$

Substituting this into (2.52) and solving the equations for $r = r_+$ and $r = r_-$ yields

$$\begin{aligned} a_+(q^2) &= -\frac{r_+(1-r_-)I(r_+) - r_-(1-r_+)I(r_-)}{r_+ - r_-}, \\ a_-(q^2) &= \frac{r_+(1+r_-)I(r_+) - r_-(1+r_+)I(r_-)}{r_+ - r_-}, \end{aligned} \quad (2.54)$$

in analog to Eq.(2.35) for $f_\pm(q^2)$. In order to illustrate several subtle points in the derivation of $I(r)$, we will go through the calculation in a bit more details. First of all, it is straightforward to show that for $P = (q_1\bar{q})$ and $V = (q_2\bar{q})$

$$\langle V|A^+|P\rangle = \int \frac{dx d^2k_\perp}{2(2\pi)^3} \frac{-2x'}{\sqrt{\mathcal{A}_P^2 + k_\perp^2} \sqrt{\mathcal{A}_V^2 + k_\perp'^2}} \phi_V^*(x', k'_\perp) \phi_P(x, k_\perp) (a + b), \quad (2.55)$$

where $\mathcal{A}_P = \mathcal{A}_1$, $\mathcal{A}_V = \mathcal{A}_2$ [see Eq.(2.41)], and

$$\begin{aligned} a &= m_1(\hat{\varepsilon} \cdot p_2 p_q^+ + \hat{\varepsilon} \cdot p_{\bar{q}} p_2^+) + m_2(\hat{\varepsilon} \cdot p_1 p_q^+ - \hat{\varepsilon} \cdot p_{\bar{q}} p_1^+) + m_{\bar{q}}(\hat{\varepsilon} \cdot p_2 p_1^+ + \hat{\varepsilon} \cdot p_1 p_2^+), \\ b &= \frac{\hat{\varepsilon} \cdot (p_2 - p_{\bar{q}})}{W_V} (m_1 m_{\bar{q}} p_2^+ - m_2 m_{\bar{q}} p_1^+ - m_1 m_2 p_q^+ + p_1 \cdot p_{\bar{q}} p_2^+ - p_1 \cdot p_2 p_q^+ + p_2 \cdot p_{\bar{q}} p_1^+), \end{aligned} \quad (2.56)$$

with $\hat{\varepsilon}^\mu = \varepsilon^\mu(\pm 1)$ given by (2.47) and $W_V = M_{0V} + m_2 + m_{\bar{q}}$. By virtue of (2.36) we find that

$$\begin{aligned} a &= (1-r)(1-2x')\mathcal{A}_P(\vec{\varepsilon}_\perp \cdot \vec{P}_\perp)P_1^+ + \dots, \\ b &= -2(1-r)\frac{\mathcal{A}_P\mathcal{B}_V + k_\perp'^2}{W_V}(\vec{\varepsilon}_\perp \cdot \vec{P}_\perp)P_1^+ + \dots, \end{aligned} \quad (2.57)$$

with

$$\mathcal{B}_V = -m_2 x' + (1-x')m_{\bar{q}}. \quad (2.58)$$

The ellipses in (2.57) denote contributions from terms proportional to $\vec{\varepsilon}_\perp \cdot \vec{k}_\perp$ in (2.56). Naively, these terms linear in \vec{k}_\perp are not expected to make contributions after integrating over \vec{k}_\perp . But this is not the case. Consider the term

$$\tilde{\phi}_V = \frac{\phi_V(x', k'_\perp)}{\sqrt{\mathcal{A}_V^2 + k_\perp'^2}} \quad (2.59)$$

and note that k'_\perp is different from k_\perp due to a non-vanishing P_\perp :

$$k'_\perp = k_\perp + (x' - x)P_\perp, \quad (2.60)$$

where we have used (2.36) and (2.37). Consequently,

$$\begin{aligned}
\tilde{\phi}_V(k'^2_\perp) &= \tilde{\phi}_V(k^2_\perp) + (d\tilde{\phi}_V/dk^2_\perp)(k'^2_\perp - k^2_\perp) + \dots \\
&= \tilde{\phi}_V(k^2_\perp) \left[1 + 2\Theta_V(x' - x)\vec{k}_\perp \cdot \vec{P}_\perp + \dots \right],
\end{aligned} \tag{2.61}$$

with

$$\Theta_V \equiv \frac{1}{\tilde{\phi}_V} \left(\frac{d\tilde{\phi}_V}{dk^2_\perp} \right). \tag{2.62}$$

Since

$$\int d^2k_\perp (\vec{\varepsilon}_\perp \cdot \vec{k}_\perp) (\vec{k}_\perp \cdot \vec{P}_\perp) = \frac{1}{2} \int d^2k_\perp k^2_\perp (\vec{\varepsilon}_\perp \cdot \vec{P}_\perp), \tag{2.63}$$

it is evident that the linear term $(\vec{\varepsilon}_\perp \cdot \vec{k}_\perp)$ in (2.57) will combine with the linear term $(\vec{k}_\perp \cdot \vec{P}_\perp)$ in (2.61) to make a contribution to $\langle V|A^+|P\rangle$. We wish to stress that this additional contribution from Θ_V was first noticed and obtained by O'Donnell and Xu [7,9] and was neglected in the work of Jaus [6,10].

By the same token, in the expression of b , the $(\vec{\varepsilon}_\perp \cdot \vec{k}_\perp)$ term in $\hat{\varepsilon} \cdot (p_2 - p_{\bar{q}})$ will also combine with the $(\vec{k}_\perp \cdot \vec{P}_\perp)$ term in $(m_1 m_{\bar{q}} p_2^+ + \dots)$ to yield a contribution proportional to $\vec{\varepsilon}_\perp \cdot \vec{P}_\perp$ after integration over k_\perp . The final result is

$$\begin{aligned}
I(r) &= - \int_0^r dx \int \frac{d^2k_\perp}{2(2\pi)^3} \frac{x' \phi_V^*(x', k_\perp) \phi_P(x, k_\perp)}{\sqrt{\mathcal{A}_P^2 + k_\perp^2} \sqrt{\mathcal{A}_V^2 + k_\perp^2}} \left\{ (1 - 2x') \mathcal{A}_P \right. \\
&\quad \left. + [(1 - 2x') \mathcal{A}_P - \mathcal{A}_V] \Theta_V(x', k_\perp) k_\perp^2 - 2 \frac{(\mathcal{A}_P \mathcal{B}_V + k_\perp^2)(1 + \Theta_V(x', k_\perp) k_\perp^2) + \frac{1}{2} k_\perp^2}{W_V} \right\}, \tag{2.64}
\end{aligned}$$

with $x' = x/r$. In deriving (2.64) we have first integrated out x' and k'_\perp . We can of course alter the order of integration by first integrating over x and k_\perp and obtain

$$\begin{aligned}
I(r) &= - \int_0^1 dx' \int \frac{d^2k_\perp}{2(2\pi)^3} \frac{x \phi_V^*(x', k_\perp) \phi_P(x, k_\perp)}{\sqrt{\mathcal{A}_P^2 + k_\perp^2} \sqrt{\mathcal{A}_V^2 + k_\perp^2}} \\
&\quad \times \left\{ \mathcal{A}_V - [(1 - 2x') \mathcal{A}_P - \mathcal{A}_V] \Theta_P(x, k_\perp) k_\perp^2 + 2 \frac{(\mathcal{A}_P \mathcal{B}_V + k_\perp^2) \Theta_P(x, k_\perp) k_\perp^2 + \frac{1}{2} k_\perp^2}{W_V} \right\}, \tag{2.65}
\end{aligned}$$

with $x = x'r$, where we have used the notation k_\perp instead of k'_\perp as it is a dummy variable. The result (2.65) will be utilized in Sec. 3 to show that light-front model calculations fulfill the heavy-quark-symmetry requirement (2.51).

At $q^2 = 0$, we have $r_+ = 1$ and $r_- = (M_V/M_P)^2$. It follows from (2.54) and (2.64) that

$$\begin{aligned}
A_2(0) &= (M_P + M_V)a_+(0) = -(M_P + M_V)I(r=1) \\
&= \int_0^1 dx \int \frac{d^2 k_\perp}{2(2\pi)^3} \frac{x\phi_V^*(x, k_\perp)\phi_P(x, k_\perp)}{\sqrt{\mathcal{A}_P^2 + k_\perp^2}\sqrt{\mathcal{A}_V^2 + k_\perp^2}} (M_P + M_V) \left\{ (1-2x)\mathcal{A}_P \right. \\
&\quad \left. + [(1-2x)\mathcal{A}_P - \mathcal{A}_V]\Theta_V(x, k_\perp)k_\perp^2 - 2\frac{(\mathcal{A}_P\mathcal{B}_V + k_\perp^2)(1 + \Theta_V(x, k_\perp)k_\perp^2) + \frac{1}{2}k_\perp^2}{W_V} \right\}.
\end{aligned} \tag{2.66}$$

This is in agreement with Eq.(30) of [9], but disagrees with the result obtained by Jaus [6].

Having fixed $a_\pm(q^2)$, we are ready to calculate $f(q^2)$ in (2.48). From (2.49) it is clear that once $f(q^2)$ is determined, so are the form factors $A_1(q^2)$ and $A_0(q^2)$. Since the “+” component of ε^μ is needed to extract $f(q^2)$, we consider the longitudinal polarization $\varepsilon^\mu(0)$ of the vector meson V and take a frame where $P_\perp = 0$. Hence,

$$-\langle V|A^+|P\rangle = f(q^2)\frac{r}{M_V}P_1^+ + \frac{r}{2M_V}\left(M_P^2 - \frac{M_V^2}{r^2}\right)[a_+(1+r) + a_-(1-r)]P_1^+. \tag{2.67}$$

Let $\langle V|A^+|P\rangle \equiv J(q^2)P_1^+$, then

$$f(q^2) = -\frac{1}{2}\left(M_P^2 - \frac{M_V^2}{r^2}\right)[a_+(1+r) + a_-(1-r)] - \frac{M_V}{r}J(q^2). \tag{2.68}$$

After a straightforward manipulation, we obtain

$$J(q^2) = -r \int_0^r dx \int \frac{d^2 k_\perp}{2(2\pi)^3} \frac{x'\phi_V^*(x', k_\perp)\phi_P(x, k_\perp)}{\sqrt{\mathcal{A}_P^2 + k_\perp^2}\sqrt{\mathcal{A}_V^2 + k_\perp^2}} (c + d), \tag{2.69}$$

with

$$\begin{aligned}
c &= -\frac{2}{M_{0V}} \left[(1-x')\frac{x'}{x}M_{0V}^2\mathcal{A}_P + \frac{m_2m_{\bar{q}}}{x}\mathcal{A}_P + k_\perp^2(m_1 + \frac{m_2}{x} - m_{\bar{q}}) \right], \\
d &= \frac{1}{M_{0V}} \frac{1}{xW_V} (\mathcal{A}_P\mathcal{B}_V + k_\perp^2) \left[-(1-2x')M_{0V}^2 + \frac{m_2^2 + k_\perp^2}{1-x'} - \frac{m_{\bar{q}}^2 + k_\perp^2}{x'} \right],
\end{aligned} \tag{2.70}$$

and [cf. Eq.(2.8)]

$$M_{0V}^2 = \frac{m_2^2 + k_\perp^2}{1-x'} + \frac{m_{\bar{q}}^2 + k_\perp^2}{x'}. \tag{2.71}$$

To check the above results, we note that for $r_+(0) = 1$ [see (2.33)]

$$\langle V|A^+|P\rangle\Big|_{r(0)=r_+(0)} = -[f(0) + (M_P^2 - M_V^2)a_+(0)]P_1^+/M_V = 2A_0(0)P_1^+, \tag{2.72}$$

so that

$$A_0(0) = \frac{1}{2}J(0)\Big|_{r=1} \tag{2.73}$$

where use has been made of (2.49). Then it is not difficult to show from (2.69-2.70) that

$$A_0(0) = \int \frac{dx d^2 k_\perp}{2(2\pi)^3} \frac{\mathcal{A}_P \mathcal{A}_V + (1-2x)k_\perp^2 + \frac{2(m_1+m_2)xk_\perp^2}{W_V}}{\sqrt{\mathcal{A}_P^2 + k_\perp^2} \sqrt{\mathcal{A}_V^2 + k_\perp^2}} \quad (2.74)$$

which agrees with Eq.(27) of [9] obtained in the $q^+ = 0$ frame (implying $r = 1$). It will be shown in Sec. III.B that our result for $f(q^2)$ does respect the heavy-quark-symmetry requirement.

Thus far we have imposed the condition $q_\perp = 0$ to extract the form factors $a_\pm(q^2)$ and $f(q^2)$. For the vector form factor $g(q^2)$ or $V(q^2)$, it proves more convenient to first let $q_\perp \neq 0$ and then set it to zero after the vector form factor is obtained. The “+” component of the vector matrix element for transverse polarization reads

$$\begin{aligned} \langle V|V^+|P \rangle &= ig\epsilon_{+\nu\alpha\beta}\epsilon^\nu P_V^\alpha P_1^\beta \\ &= ig\epsilon_{+-xy}[-\epsilon^- q^x P^y + (P_1 - P_V)^- \epsilon^x P^y - P_1^- \epsilon^x q^y - (x \leftrightarrow y)], \end{aligned} \quad (2.75)$$

where $P_\perp \equiv P_{1\perp}$, $P_{V\perp} = P_\perp - q_\perp$. At the quark level, we have

$$\begin{aligned} \langle V|V^+|P \rangle &= \int_0^r dx \int \frac{d^2 k_\perp}{2(2\pi)^3} \frac{2x' \phi_V^*(x', k_\perp) \phi_P(x, k_\perp)}{\sqrt{\mathcal{A}_P^2 + k_\perp^2} \sqrt{\mathcal{A}_V^2 + k_\perp^2}} \left[\frac{\hat{\epsilon} \cdot (p_2 - p_{\bar{q}})}{W_V} i\epsilon_{+\alpha\beta\gamma} p_2^\alpha p_1^\beta p_{\bar{q}}^\gamma \right. \\ &\quad \left. + i\epsilon_{+\alpha\beta\gamma} \hat{\epsilon}^\alpha (m_1 p_2^\beta p_{\bar{q}}^\gamma - m_2 p_1^\beta p_{\bar{q}}^\gamma + m_{\bar{q}} p_2^\beta p_1^\gamma) \right]. \end{aligned} \quad (2.76)$$

The transverse momentum variables are

$$p_{1\perp} = (1-x)P_\perp + k_\perp, \quad p_{2\perp} = (1-x)P_\perp - q_\perp + k_\perp, \quad p_{\bar{q}\perp} = xP_\perp - k_\perp. \quad (2.77)$$

It suffices to set $\hat{\epsilon}^\mu = \epsilon^-(\pm)$ in (2.76) to get contributions proportional to $\epsilon_{+-xy}\epsilon^-(q^x p^y - q^y p^x)$, which is related to the first term of (2.75) at the hadron level. It is easy to check that the transverse components $\hat{\epsilon}^x(\pm)$ and $\hat{\epsilon}^y(\pm)$ will not generate the same structure. Repeating the similar derivation as before, we obtain

$$\begin{aligned} g(q^2) &= \frac{2V(q^2)}{M_P + M_V} = \int_0^r dx \int \frac{d^2 k_\perp}{2(2\pi)^3} \frac{2x' \phi_V^*(x', k_\perp) \phi_P(x, k_\perp)}{\sqrt{\mathcal{A}_P^2 + k_\perp^2} \sqrt{\mathcal{A}_V^2 + k_\perp^2}} \\ &\quad \times \left\{ \mathcal{A}_P + (\mathcal{A}_P - \mathcal{A}_V) \Theta_V(x', k_\perp) k_\perp^2 + \frac{1}{W_V} \left[r k_\perp^2 + (1-r) \left(2x M_{0P} k_z - \frac{x' k_\perp^2}{1-x'} \right) \right. \right. \\ &\quad \left. \left. + (1-r) \Theta_V(x', k_\perp) k_\perp^2 (2x^2 M_{0P}^2 - x'^2 M_{0V}^2 - m_{q'}^2 - k_\perp^2) \right] \right\}, \end{aligned} \quad (2.78)$$

with k_z being defined in (2.17). For $r(0) = r_+(0) = 1$, (2.78) leads to

$$V(0) = \int_0^1 dx \int \frac{d^2 k_\perp}{2(2\pi)^3} \frac{(M_P + M_V)x\phi_V^*(x', k_\perp)\phi_P(x, k_\perp)}{\sqrt{\mathcal{A}_P^2 + k_\perp^2}\sqrt{\mathcal{A}_V^2 + k_\perp^2}} \times \left(\mathcal{A}_P + \frac{k_\perp^2}{W_V} + x(m_1 - m_2)\Theta_V(x, k_\perp)k_\perp^2 \right), \quad (2.79)$$

which agrees with [9].

Therefore, we have calculated the form factors $f(q^2)$, $g(q^2)$ and $a_\pm(q^2)$ in the time-like q^2 region within the light-front framework. Form factors $V(q^2)$ and $A_{0,1,2}(q^2)$ can then be determined via Eq.(2.49).¹

D. Non-valence Contribution

Thus far we have concentrated on the valence-quark contribution to the form factors. As stated in the Introduction, there also exist contributions which are generated from the quark-antiquark excitation or higher Fock-states in the hadronic bound states. This additional Z -graph contribution vanishes in the frame where the momentum transfer is purely transverse i.e., $q^+ = 0$, but survives otherwise.

The general feature of the non-valence configuration can be recognized by considering the quark triangle diagram (see Fig. 1). In terms of the “+” component of momenta, the Feynman triangle diagram in the light-front framework consists of two subprocesses: one corresponds to the valence-quark approximation for the meson wave functions, and the other to the contribution of quark-pair creation from the vacuum. That is, through the mechanism of quark-antiquark pair creation, the “spectator” quark in the second subprocess is fragmented into a meson plus an outgoing quark. A detailed study of the quark triangle diagram for $P \rightarrow P$ transition gives (generalization to $P \rightarrow V$ transition is straightforward) [13]

$$\langle P_2 | \bar{q}_2 \gamma^+ q_1 | P_1 \rangle = \mathcal{M}_a^+ + \mathcal{M}_b^+, \quad (2.80)$$

¹In the frame where $q^+ = 0$, only three of the $P \rightarrow V$ form factors, namely f , g and a_+ or V , A_1 and A_2 are determined. However, A_0 can be fixed at $q^2 = 0$ using the relation $A_0(0) = A_3(0)$ and (2.46).

with

$$\begin{aligned}\mathcal{M}_a^+ &= g_1 g_2 \int_0^r \frac{dx}{x(1-x)(1-x')} \int \frac{d^2 k_\perp}{2(2\pi)^3} \frac{N_a^+}{(M_1^2 - M_{01}^2)(M_2^2 - M_{02}^2)}, \\ \mathcal{M}_b^+ &= -g_1 g_2 \int_r^1 \frac{dx}{x(1-x)(1-x')} \int \frac{d^2 k_\perp}{2(2\pi)^3} \frac{N_b^+}{(M_1^2 - M_{01}^2)(q^2 - M_{12}^2) \frac{r}{1-r}},\end{aligned}\quad (2.81)$$

where $x' = x/r$, g_1 and g_2 are the quark-meson coupling constants at different vertices, M_1 and M_2 are the masses of the initial and final meson respectively, M_{01}^2 (M_{02}^2) is the same as M_{0P}^2 (M_{0V}^2) defined in (2.71), and

$$\begin{aligned}M_{12}^2 &= \left(\frac{m_1^2 + k_\perp^2}{1-x} - \frac{m_2^2 + k_\perp^2}{r-x} \right) (1-r), \\ N_a^+ &= 4[p_1^+(m_2 m_{\bar{q}} + p_2 \cdot p_{\bar{q}}) + p_2^+(m_1 m_{\bar{q}} + p_1 \cdot p_{\bar{q}}) + p_{\bar{q}}^+(m_1 m_2 - p_1 \cdot p_2)], \\ N_b^+ &= 4[p_1^+(-\eta M_1 m_2 + P_1 \cdot p_2) + p_2^+(-\eta M_1 m_1 + P_1 \cdot p_1) + P_1^+(m_1 m_2 - p_1 \cdot p_2)],\end{aligned}\quad (2.82)$$

with $\eta = (m_1 - m_{\bar{q}})/M_1$. Since \mathcal{M}_a receives contributions from the kinematic region $0 < x < r$ or $0 < k^+ < P_2^+$ (see Fig. 1), it corresponds to the valence-quark configuration. As for \mathcal{M}_b^+ , only the region $r < x < 1$ or $P_2^+ < k^+ < P_1^+$ is relevant, and it corresponds to the non-valence contribution. It is straightforward to check that, apart from a sign difference, N_a^+ is precisely the trace term given in (2.40). This implies that the previous calculation for $P \rightarrow P$ form factors in the Hamiltonian light-front approach is identical to the Feynman triangle graph under the valence-quark approximation. Obviously, making the following substitutions

$$\begin{aligned}\frac{\sqrt{2}g_1}{x(1-x)} \frac{1}{M_1^2 - M_{01}^2} &\longrightarrow \frac{\phi_1(x, k_\perp)}{\sqrt{\mathcal{A}_1^2 + k_\perp^2}}, \\ \frac{\sqrt{2}g_2}{x'(1-x')} \frac{1}{M_2^2 - M_{02}^2} &\longrightarrow \frac{\phi_2(x', k_\perp)}{\sqrt{\mathcal{A}_2^2 + k_\perp^2}}\end{aligned}\quad (2.83)$$

in \mathcal{M}_a^+ will reproduce the result $\langle P_2 | \bar{q}_2 \gamma^+ q_1 | P_1 \rangle = 2P_1^+ H$ [see (2.34) and (2.43)].

Unlike the valence-quark contribution, only the wave function $\phi_1(x, k_\perp)$ of the initial meson enters into the expression of \mathcal{M}_b^+ ; $\phi_2(x', k_\perp)$ is not applicable for the non-valence graph because the light-front momentum k^+ of the spectator quark is larger than the momentum P_2^+ of the daughter meson (see Fig. 1). This makes the task of calculating the effect of the Z -graph considerably more difficult. Nevertheless, some qualitative features of \mathcal{M}_b^+ can still be comprehended. First of all, as noted earlier, the contribution from non-valence

configurations vanishes in a frame where $q^+ = 0$ or $r = 1$. However, this frame is suitable only for space-like q^2 . Second, it is easy to show that $N_b^+ \rightarrow 0$ in the limit of heavy quark symmetry $m_Q \rightarrow \infty$, because it takes an infinite amount of energy to create a heavy quark-antiquark pair. This has the important implication that we do not have to worry about the pair-creation subprocess when calculating the Isgur-Wise function. Beyond the heavy-quark limit, it is commonly argued that the non-valence contribution leads to a small correction in heavy-to-heavy transition but becomes more important for heavy-to-light decays [15,10,13]. For example, a B^* -pole contribution is usually believed to be the dominant non-valence effect in $B \rightarrow \pi$ transition, especially when q^2 is near the zero-recoil point [22]. Some estimates based on the B^* -pole contribution with the help of chiral perturbation theory indicate that for large values of q^2 , the Z -graph provides the dominant contribution to $B \rightarrow \pi$ form factors (for a recent estimate, see [12]).

In this paper we will demonstrate that even for heavy-to-heavy transition, the importance of the non-valence contribution depends on the recoiling direction of the daughter meson. As shown in (2.31), for a given q^2 there are two possible reference frames characterized by $r_+(q^2)$ and $r_-(q^2)$, corresponding to whether one chooses the velocity of the final meson to be in the positive or negative z -direction relative to the initial meson. Of course, the form factors are independent of the choice of the “+” or “−” frame. This means that the combination $\mathcal{M}_a^+ + \mathcal{M}_b^+$ in (2.80) should be independent of the choice of $r(q^2) = r_+(q^2)$ or $r(q^2) = r_-(q^2)$. From (2.81) we see that the r dependence of \mathcal{M}_a^+ or \mathcal{M}_b^+ appears both in the integrand and in the integration limit. As a consequence, \mathcal{M}_a^+ and \mathcal{M}_b^+ separately are in general “ \pm ”-frame dependent. In other words, *the valence-quark and non-valence contributions to mesonic form factors are in general dependent on the recoiling direction of the final meson, but their sum is not*. For the form factors $f_\pm(q^2)$ in $P \rightarrow P$ decay and $a_\pm(q^2)$ in $P \rightarrow V$ transition, we have “demanded” that the valence contribution itself be frame independent [see (2.34), (2.35) and (2.54)]. For form factors A_0 , A_1 and V in $P \rightarrow V$ decay, explicit calculations in Sec. IV.B show that the valence contributions for $r = r_+$ and $r = r_-$ are indeed different (see Fig. 6). Thus in principle we cannot make firm predictions for these form factors even for $B \rightarrow D^*$ transition, unless the non-valence contributions are also calculated. Nevertheless, corrections due to the non-valence configuration are expected to be marginal for heavy-to-heavy form factors evaluated in the “+” frame where $r = r_+$, but become more significant in the “−”

frame ($r = r_-$). The argument goes as follows: we know that the non-valence contribution vanishes if $q^+ = 0$. Now q^+ is never zero in the “−” frame, whereas in the “+” frame $q^+ = 0$ when $r_+ = 1$ [see (2.33)]. That means the valence-quark contribution in the “+” frame is *exact* at the $q^2 = 0$ point. As will be shown in Sec. IV.B, the valence contributions at $q^2 = 0$ in the “−” frame are generally smaller than those in the “+” frame; the difference should be accounted for by the non-valence configuration. These points will be elucidated in more detail in Sec. IV.B.

III. THE ISGUR-WISE FUNCTION

In Sec. 2 we have computed the $P \rightarrow P$ form factors $f_{\pm}(q^2)$ and $P \rightarrow V$ form factors $V(q^2)$, $A_{0,1,2}(q^2)$ for the entire physical q^2 region using the light-front wave functions. It is very important to check if the light-front model predictions are in accord with the requirements of heavy-quark symmetry, namely (2.29) and (2.51). In other words, as $m_Q \rightarrow \infty$, we would like to see if there exists a universal Isgur-Wise function which governs all heavy-to-heavy mesonic form factors in the light-front quark model.

To our knowledge, the Isgur-Wise function has not been calculated directly for $q^2 \geq 0$ within the framework of the light-front quark model, though it has been considered in [9,19,11]. The analysis of [9] is based on the observation [20] that the knowledge of $P \rightarrow P$ or $P \rightarrow V$ form factors at $q^2 = 0$ (or at any point of q^2) suffices to determine the Isgur-Wise function in the whole kinematic region. However, this relies on the assumption that the model calculations of form factors obey heavy-quark symmetry and that the universal form factor is only a function of $v \cdot v'$. The Isgur-Wise function is derived in [19] from *space-like elastic* form factors of heavy mesons,² while it is obtained in [11] by performing an analytic continuation from the region $q^2 \leq 0$ to time-like momentum transfers. In contrast, we do not impose heavy-quark symmetry from the outset, so that we can check explicitly if the weak decay form factors of heavy mesons can indeed be described by a single universal function when $m_Q \rightarrow \infty$. We will calculate this universal function directly at the time-like momentum

²This is based on the argument that, for the elastic form factor, $q^2 = -(v \cdot v' - 1)/(2M)$. Thus the space-like elastic form factor is related to the Isgur-Wise function at time-like momentum transfers ($v \cdot v' \geq 1$).

transfer to see if it is independent of heavy quark masses and their ratio. It is important to note that, since heavy quark-pair creation is forbidden in the $m_Q \rightarrow \infty$ limit, the Z -graph is no longer a problem in the reference frame where $q^+ \geq 0$. Therefore, within the light-front quark model, we are able to compute the Isgur-Wise function *exactly* for time-like q^2 .

To proceed, we first investigate the heavy-quark-limit behavior of the wave function. In the infinite quark mass limit $m_Q \rightarrow \infty$, the light-front wave function has the scaling behavior [17]:

$$\phi_{Q\bar{q}}(x, k_\perp) \rightarrow \sqrt{m_Q} \Phi(m_Q x, k_\perp), \quad (3.1)$$

where the factor $\sqrt{m_Q}$ or \sqrt{M} (M being the mass of the heavy meson) comes from the particular normalization we have assumed for the physical state in (2.12-2.13). The reason why the light-front heavy-meson wave function should have such an asymptotic form is as follows. Since x is the longitudinal momentum fraction carried by the light antiquark, the meson wave function should be sharply peaked near $x \sim \Lambda_{\text{QCD}}/m_Q$. It is thus clear that only terms of the form “ $m_Q x$ ” survive in the wave function as $m_Q \rightarrow \infty$; that is, $m_Q x$ is independent of m_Q in the $m_Q \rightarrow \infty$ limit. For the BSW wave function (2.14), we find that

$$\Phi(X, k_\perp)_{\text{BSW}} = \sqrt{32} \left(\frac{\pi}{\omega^2} \right) \exp \left(-\frac{k_\perp^2}{2\omega^2} \right) \exp \left(-\frac{X^2}{2\omega^2} \right) \sqrt{X}, \quad (3.2)$$

where $X \equiv m_Q x$, and the normalization condition (2.13) becomes

$$\int_0^\infty dX \int \frac{d^2 k_\perp}{2(2\pi)^3} |\Phi(X, k_\perp)|^2 = 1. \quad (3.3)$$

For the Gaussian-type wave function (2.15), we obtain

$$\Phi(X, k_\perp)_{\text{Gauss}} = 4 \left(\frac{\pi}{\omega^2} \right)^{3/4} \exp \left(-\frac{\vec{k}_\perp^2}{2\omega^2} \right) \sqrt{\frac{dk_z}{dX}}. \quad (3.4)$$

From (2.17) it is clear that $k_z = [X - (m_q^2 + k_\perp^2)/X]/2$ in the heavy-quark limit. Therefore,

$$\Phi(X, k_\perp)_{\text{Gauss}} = 4 \left(\frac{\pi}{\omega^2} \right)^{3/4} \exp \left(-\frac{k_\perp^2}{2\omega^2} \right) \exp \left(-\frac{(\frac{X}{2} - \frac{m_q^2 + k_\perp^2}{2X})^2}{2\omega^2} \right) \sqrt{\frac{1}{2} + \frac{m_q^2 + k_\perp^2}{2X^2}}. \quad (3.5)$$

However, since $M_0 \rightarrow m_Q + \mathcal{O}(m_Q x)$, it is clear that the wave function (2.19), which is a variant of the Gaussian type, does not have the correct asymptotic form in the heavy-quark limit. Hence it is not suitable for describing heavy-quark transitions.

A. $P \rightarrow P$ Transition in Heavy-Quark Limit

With the light-front wave function $\Phi(X, k_\perp)$ constructed in the $m_Q \rightarrow \infty$ limit, the $P \rightarrow P$ transition function $H(r)$ (2.43) in the limit of heavy-quark symmetry (i.e., $m_1, m_2 \rightarrow \infty$) becomes

$$H(r) = \sqrt{\frac{M_2}{M_1}} \int_0^\infty dX \int \frac{d^2 k_\perp}{2(2\pi)^3} \Phi(X', k_\perp) \Phi(X, k_\perp) \frac{\mathcal{A}(X) \mathcal{A}(X') + k_\perp^2}{\sqrt{\mathcal{A}^2(X) + k_\perp^2} \sqrt{\mathcal{A}^2(X') + k_\perp^2}}, \quad (3.6)$$

where $X \equiv m_1 x$, $X' \equiv m_2 x'$, and $\mathcal{A}(X) = X + m_{\bar{q}}$. Note that the quantities X , X' , $m_{\bar{q}}$ and k_\perp appearing in the integrand are all of order Λ_{QCD} . Denote $z \equiv v_2^+ / v_1^+ = (M_1/M_2)r$, then [see (2.31)],

$$z_\pm = v_1 \cdot v_2 \pm \sqrt{(v_1 \cdot v_2)^2 - 1}. \quad (3.7)$$

Obviously, $z_+ z_- = 1$ and $X'/X = 1/z$. Let $H(r_\pm) = \sqrt{M_2/M_1} \widetilde{H}(z_\pm)$, so that (2.34) can be rewritten as

$$\langle P_2 | V^+ | P_1 \rangle = 2\sqrt{M_1 M_2} \widetilde{H}(z) v_1^+. \quad (3.8)$$

By a simple change of integration variable, one can readily show that

$$\widetilde{H}(z) = z \widetilde{H}(1/z). \quad (3.9)$$

To check the validity of the heavy-quark-symmetry relation (2.29), we note that $h_\pm(q^2)$ are related to $\widetilde{H}(z)$ via

$$h_\pm(q^2) = \frac{1 \mp z}{1 - z^2} \left[\widetilde{H}(z) \pm z \widetilde{H}(1/z) \right], \quad (3.10)$$

in analog to (2.35) for $f_\pm(q^2)$. By virtue of (3.9), the HQS relation $h_-(q^2) = 0$ given in (2.29) is indeed satisfied, and the Isgur-Wise function is given by

$$\xi(v_1 \cdot v_2) = \frac{2\widetilde{H}(z)}{1 + z}. \quad (3.11)$$

Evidently, the Isgur-Wise function is independent of the heavy quark masses m_1, m_2 and their ratio, but it depends on the light spectator quark mass. The R.H.S. of (3.11) is invariant under the exchange $z \leftrightarrow 1/z$, implying that the Isgur-Wise function $\xi(v_1 \cdot v_2)$ is independent of the choice of the recoiling direction of the daughter meson, as it should be. At zero recoil

($z = 1$), the expression for $\widetilde{H}(1)$ becomes identical to the normalization condition (3.3). Hence $\widetilde{H}(1) = 1$, and the Isgur-Wise function obeys the correct normalization condition $\xi(1) = 1$. We would like to stress again that, unlike the previous works [9,11] where $\xi(v \cdot v')$ is actually evaluated for $B \rightarrow D$ transition and for space-like values of q^2 , here the Isgur-Wise function is obtained in the infinite quark mass limit and calculated directly for $q^2 \geq 0$. Within the specific model we have taken, our result is exact.

In the limit of heavy-quark symmetry, form factors F_1 and F_0 are related to the Isgur-Wise function via

$$\xi(v_1 \cdot v_2) = \frac{2\sqrt{M_1 M_2}}{M_1 + M_2} F_1(q^2) = \frac{2\sqrt{M_1 M_2}}{M_1 + M_2} \frac{F_0(q^2)}{\left[1 - \frac{q^2}{(M_1 + M_2)^2}\right]}. \quad (3.12)$$

Hence the q^2 dependence of F_1 is different from that of F_0 by an additional pole factor.

B. $P \rightarrow V$ Transition in Heavy-Quark Limit

There are four HQS relations given in (2.51) for $P \rightarrow V$ form factors. We shall first focus on \tilde{a}_\pm (or a_\pm). As $m_1, m_2 \rightarrow \infty$, we can show that

$$\Theta_V(x', k_\perp) \rightarrow \Theta(X', k_\perp), \quad \Theta_P(x, k_\perp) \rightarrow \Theta(X, k_\perp), \quad (3.13)$$

with Θ_V being defined in (2.61). The $P \rightarrow V$ transition amplitude $I(r)$ [see (2.64) and (2.65)] reduce to

$$\begin{aligned} I(r) = \tilde{I}(z) &= -\frac{1}{\sqrt{m_1 m_2}} \int \frac{dX d^2 k_\perp}{2(2\pi)^3} [X' \mathcal{A}(X) + X'(X - X') \Theta(X', k_\perp) k_\perp^2] f(X) f(X') \\ &= -\frac{1}{\sqrt{m_1 m_2}} \int \frac{dX' d^2 k_\perp}{2(2\pi)^3} [X \mathcal{A}(X') - X(X - X') \Theta(X, k_\perp) k_\perp^2] f(X) f(X'), \end{aligned} \quad (3.14)$$

where $f(X) = \Phi(X, k_\perp) / \sqrt{\mathcal{A}^2(X) + k_\perp^2}$, $X' = X/z$, and all terms proportional to $1/W_V$ have been neglected in the heavy-quark limit. It is evident that $\tilde{I}(z)$ satisfies the relation

$$\tilde{I}(z) = \tilde{I}(1/z). \quad (3.15)$$

Therefore, from (2.54),

$$\tilde{a}_+ + \tilde{a}_- = \frac{2M_P^2}{\sqrt{M_P M_V}} \frac{r_+ r_- \tilde{I}(z_+) - r_+ r_- \tilde{I}(z_-)}{r_+ - r_-} = 0, \quad (3.16)$$

and

$$\tilde{a}_+ - \tilde{a}_- = 2\sqrt{M_P M_V} \frac{-r_+ \tilde{I}(z_+) + r_- \tilde{I}(z_-)}{r_+ - r_-} = -2\sqrt{M_P M_V} \tilde{I}(z). \quad (3.17)$$

By comparing this with (2.51) yields the Isgur-Wise function

$$\begin{aligned} \zeta(v \cdot v') &= 2 \int_0^\infty dX \int \frac{d^2 k_\perp}{2(2\pi)^3} \frac{\Phi(X', k_\perp) \Phi(X, k_\perp)}{\sqrt{\mathcal{A}^2(X) + k_\perp^2} \sqrt{\mathcal{A}^2(X') + k_\perp^2}} \\ &\times \left\{ X' \mathcal{A}(X) + X'(X - X') \Theta(X', k_\perp) k_\perp^2 \right\}. \end{aligned} \quad (3.18)$$

with $X'/X = 1/z$. It remains to show that $\zeta(v \cdot v')$ is indeed the same as the Isgur-Wise function $\xi(v \cdot v')$ found in $P \rightarrow P$ transition (3.11). We will address this issue later in Sec. IV. After showing the HQS relations (3.16) and (3.17) for form factors \tilde{a}_\pm , we turn to the vector form factor. One can easily show from (2.78) that, indeed,

$$\tilde{g}(q^2) = \sqrt{M_P M_V} g(q^2) \xrightarrow{\text{HQ limit}} -2\sqrt{M_P M_V} \tilde{I}(z) = \zeta(v \cdot v'), \quad (3.19)$$

in accord with (2.51).

Using the results (3.16) and (3.17) for form factors \tilde{a}_\pm , we are ready to prove the remaining HQS relation for $f(q^2)$. It follows from (2.45), (2.68) and (2.69-2.70) that

$$\tilde{f}(q^2) = \frac{f(q^2)}{\sqrt{M_P M_V}} = -\frac{1}{2} \frac{X^2 - X'^2}{X X'} \zeta + \int \frac{dX d^2 k_\perp}{2(2\pi)^3} \frac{\Phi(X', k_\perp) \Phi(X, k_\perp)}{\sqrt{\mathcal{A}_P^2 + k_\perp^2} \sqrt{\mathcal{A}_V^2 + k_\perp^2}} \left(\frac{x' M_V}{m_1} c \right), \quad (3.20)$$

where terms proportional to $1/W_V$ vanish in the limit of heavy-quark symmetry. We find from (2.70) that

$$\frac{x' M_V}{m_1} c \xrightarrow{\text{HQ limit}} -2 \frac{X'}{X} (\mathcal{A}_P \mathcal{A}_V + k_\perp^2), \quad (3.21)$$

hence

$$\tilde{f}(q^2) = -\frac{1}{2} \frac{X^2 - X'^2}{X X'} \zeta(v \cdot v') - \frac{X'}{X} \left(1 + \frac{X}{X'} \right) \xi(v \cdot v'), \quad (3.22)$$

where use of (3.11) has been made. Then, using $X'/X = 1/z$ and (3.7), we are led to the desired HQS relation given in (2.51):

$$\tilde{f}(q^2) = -(1 + v \cdot v') \xi(v \cdot v'), \quad (3.23)$$

provided that $\zeta(v \cdot v') = \xi(v \cdot v')$.

Is the function $\zeta(v \cdot v')$ given by (3.18) identical to the Isgur-Wise function $\xi(v \cdot v')$? While $\xi(1) = 1$ is always valid irrespective of the details of the light-front amplitude used, the normalization of $\zeta(v \cdot v')$ at zero recoil is nontrivial. In fact, we find that $\zeta(1)$ depends on the choice of the light-front model wave function. We find numerically (see Sec. IV.A) that the HQS requirement $\zeta(1) = 1$ is fulfilled by the Gaussian-type wave function (2.15), but not so by the BSW-type wave function (2.14). In other words, *the normalization of the Isgur-Wise function at zero recoil in $P \rightarrow V$ transition puts a severe restriction on the phenomenological light-front wave functions*. Since we are not able to solve the light-front QCD bound-state equation to obtain the momentum distribution amplitude $\phi(x, k_\perp)$, we see that heavy-quark symmetry is helpful in discriminating between different phenomenological amplitudes. As will be shown in Sec. IV.A, $\zeta(v \cdot v')$ is numerically equal to $\xi(v \cdot v')$ if the Gaussian-type wave function is used.

The $P \rightarrow V$ form factors in the heavy-quark limit are all related to the Isgur-Wise function via

$$\begin{aligned}\zeta(v \cdot v') &= \frac{2\sqrt{M_P M_V}}{M_P + M_V} V(q^2) = \frac{2\sqrt{M_P M_V}}{M_P + M_V} A_0(q^2) \\ &= \frac{2\sqrt{M_P M_V}}{M_P + M_V} A_2(q^2) = \frac{2\sqrt{M_P M_V}}{M_P + M_V} \frac{A_1(q^2)}{\left[1 - \frac{q^2}{(M_P + M_V)^2}\right]}.\end{aligned}\quad (3.24)$$

That means V , A_0 , A_2 all have the same q^2 dependence and they differ from A_1 by an additional pole factor.

IV. NUMERICAL RESULTS AND DISCUSSIONS

To examine numerically the form factors derived in the last section, we need to specify the parameters appearing in the phenomenological light-front wave functions. We shall use the decay constants to constrain the quark mass m_q and the scale parameter ω . The decay constants of light pseudoscalar and vector mesons are³

$$f_\pi = 132 \text{ MeV}, \quad f_K = 160 \text{ MeV}, \quad f_\rho = 216 \text{ MeV}, \quad f_{K^*} = 210 \text{ MeV}.\quad (4.1)$$

³The decay constant f_ρ is obtained from the measured decay rate of $\rho^0 \rightarrow e^+e^-$, while f_{K^*} is determined from $\tau \rightarrow K^*\nu_\tau$.

The decay constants of heavy mesons are unknown experimentally, so we have to rely on model calculations and lattice results. To be specific, we take

$$f_D = 200 \text{ MeV}, \quad f_B = 185 \text{ MeV}, \quad f_{D^*} = 250 \text{ MeV}, \quad f_{B^*} = 205 \text{ MeV}, \quad (4.2)$$

where the estimates for f_{D^*} and f_{B^*} are relatively more uncertain. The parameters m_q and ω in the Gaussian-type and BSW-type wave functions fitted to the decay constants via (2.21) and (2.24) are listed in Table I. Note that the quark masses given in Table I are fixed to the commonly used values, and the other fitted values are by no means unique. Presumably, other hadronic properties, for example the light-meson elastic form factor measured at a wide range of momentum transfer, would be helpful in fixing the light-front parameters.

Table I. Parameters m_q (in units of GeV) and ω in the Gaussian-type and BSW-type wave functions fitted to the decay constants given by (4.1) and (4.2).

wave function	$m_{u,d}$	ω_π	ω_ρ	m_s	ω_K	ω_{K^*}	m_c	ω_D	ω_{D^*}	m_b	ω_B	ω_{B^*}
Gaussian	0.25	0.33	0.30	0.40	0.38	0.31	1.6	0.46	0.47	4.8	0.55	0.55
BSW	0.25	0.30	0.29	0.40	0.34	0.30	1.6	0.46	0.46	4.8	0.58	0.57

A. Results for the Isgur-Wise function

Before proceeding to numerically evaluate the $P \rightarrow P$ and $P \rightarrow V$ form factors, it is important to check the Isgur-Wise function to ensure that model calculations do respect heavy-quark symmetry in the infinite quark mass limit. With the Gaussian-type (3.4) and BSW-type (3.2) wave functions given in the limit of heavy-quark symmetry, the Isgur-Wise function $\xi(v \cdot v')$ for $P \rightarrow P$ transition calculated from (3.11) and (3.10) is shown in Fig. 2 using $\omega_D = \omega_B = 0.55$. We see that the Isgur-Wise function obtained from Gaussian-type and BSW wave functions is very similar. The slope of $\xi(v \cdot v')$ at the zero-recoil point is

$$\rho^2 \equiv -\xi'(1) = 1.24. \quad (4.3)$$

Recent theoretical estimates and experimental analyses favor $\rho^2 \lesssim 1$. The slope parameter ρ^2 is subject to constraints from Bjorken and Voloshin sum rules (for a review, see [2]). A tight bound is derived to be $0.5 < \rho^2 < 0.8$ [21]. QCD sum-rule results range from 0.70 to 1.00 [21]. It thus appears that our slope parameter (4.3) is too large. This may be attributed to

the fact that the Gaussian-type amplitude does not have enough amount of high-momentum components at large k_\perp . It has been shown in [19] that the one-gluon-exchange interaction can generate high-momentum components in the meson wave function and reduce the value of ρ^2 significantly.

Although ξ is independent of heavy quark masses, it is interesting to see if it can be fitted to a simple pole behavior for a specific transition, e.g., $B \rightarrow D$:

$$\xi(q^2) = \frac{\xi(0)}{(1 - q^2/M_{\text{pole}}^2)^\alpha}, \quad (4.4)$$

where $v \cdot v' = (M_B^2 + M_D^2 - q^2)/(2M_B M_D)$. We find that $\xi(q^2)$ is fitted very well over the entire $q^2 \geq 0$ region with a dipole behavior (one cannot tell the difference between fitted and calculated curves) with

$$\alpha = 2, \quad M_{\text{pole}} = 6.65 \text{ GeV}. \quad (4.5)$$

Indeed, this pole mass is close to the mass 6.34 GeV of the 1^+ vector meson with $(b\bar{c})$ content.

The most interesting and striking results are shown in Fig. 3 for the function $\zeta(v \cdot v')$ [see (3.18)] for $P \rightarrow V$ transition obtained by taking the heavy-quark limit of the form factor $A_2(q^2)$ or $V(q^2)$. For the Gaussian-type wave function, we find that $\zeta(1) = 1$ at zero recoil, and that numerically $\zeta(v \cdot v')$ is identical to $\xi(v \cdot v')$.⁴ In contrast, the curve computed using the BSW amplitude deviates consistently from $\xi(v \cdot v')$; in particular, $\zeta(1) = 0.87$ at zero-recoil. That means, for reasons not clear to us, the overlapping of the BSW wave functions for $P \rightarrow V$ transition at zero recoil is not complete in the heavy-quark limit. This in turn implies that the light-front amplitude Φ_{BSW} is inconsistent with heavy-quark symmetry for $P \rightarrow V$ transition.

We note that the presence of the Θ term in (3.18) is crucial for obtaining the numerical equivalence of $\zeta(v \cdot v')$ and $\xi(v \cdot v')$. Hence the form factors $V(q^2)$, $A_1(q^2)$, $A_2(q^2)$ obtained previously in [6,10] are incomplete since the Θ terms are not taken into account there.

⁴Since numerically $\zeta(v \cdot v')$ is equal to $\xi(v \cdot v')$ up to six digits for the Gaussian-type amplitude, we believe that this equivalence is *exact*, although both Maple and Mathematica fail to give an analytic result for (3.18).

B. $P \rightarrow P$ Form Factors

Since the BSW wave function fails to give a correct normalization at zero recoil for the Isgur-Wise function in $P \rightarrow V$ transition, the ensuing calculations are all carried out using the Gaussian-type wave function. The q^2 dependence of the form factors $F_1(q^2) = f_+(q^2)$ and $F_0(q^2)$ for $B \rightarrow D$ weak transition computed using (2.28), (2.35) and (2.43) are shown in Fig. 4 (we have neglected the non-valence contributions). At $q^2 = 0$, we obtain $F_1^{BD}(0) = F_0^{BD}(0) = 0.70$. From Fig. 4 we see that $F_1^{BD}(q^2)$ can be fitted by a dipole approximation in the entire time-like q^2 region with a pole mass $M_{\text{pole}} = 6.59$ GeV, in agreement with the pole mass 6.65 GeV fitted to the Isgur-Wise function [cf. (4.5)], while $F_0^{BD}(q^2)$ at low q^2 ($0 \leq q^2 \lesssim 6 \text{ GeV}^2$) exhibits a monopole dependence with $M_{\text{pole}} = 7.90$ GeV. This monopole behavior for F_0^{BD} at low q^2 is consistent with (3.12).

The q^2 dependence of the form factor $f_+(q^2)$ for the transitions $B \rightarrow \pi$, $B \rightarrow K$, $D \rightarrow \pi$ and $D \rightarrow K$ are shown in Fig. 5. The numerical results for the form factors at $q^2 = 0$ are

$$f_+^{B\pi}(0) = 0.29, \quad f_+^{BK}(0) = 0.34, \quad f_+^{D\pi}(0) = 0.64, \quad f_+^{DK}(0) = 0.75. \quad (4.6)$$

From Fig. 5 we see that, near the zero-recoil point, the valence-quark prediction for $f_+^{B\pi}$ decreases as q^2 increases. As explained in [12], the dipping of the valence-quark contribution toward the q_{max}^2 point can be understood as follows. Recall that the decay amplitude involves an overlapping integral of the wave functions of the initial and final mesons. If both mesons were heavy, then it is obvious that, by heavy-quark symmetry, maximum overlapping must occur at the zero-recoil point. However, in the situation of $B \rightarrow \pi$ transition, the internal momentum distributions of the heavy B meson and light pion peak at different values of x . Specifically, $\phi_B(x, k_\perp)$ has a narrow peak near $x = 0$, whereas $\phi_\pi(x, k_\perp)$ peaks with a much larger width at $x = 1/2$. Consequently, maximum overlapping of the wave functions actually occurs somewhat away from the zero-recoil kinematics. For $D \rightarrow \pi$ transition, maximum overlapping occurs in the close vicinity of zero recoil (see Fig. 5). Since the non-valence contribution is expected to be important for heavy-to-light form factors, especially for $B \rightarrow \pi$ transition, a comparison with data at large q^2 cannot be made until such contribution is included (form factors at $q^2 = 0$ are not affected by the pair-creation configuration).⁵

⁵In [11] form factors at $q^2 \leq 0$ are reformulated as a double dispersion integral representation,

We see from (4.6) that while the predicted $f_+^{DK}(0)$ is in nice agreement with experiment, $f_+^{DK}(0)_{\text{expt}} = 0.75 \pm 0.03$ [23]; $f_+^{D\pi}(0)$ and the ratio $R = f_+^{D\pi}(0)/f_+^{DK}(0) = 0.87$ are too small compared to the measured values $R = 1.29 \pm 0.21 \pm 0.11$ [24] and $1.01 \pm 0.20 \pm 0.07$ [25]. It has been pointed out in [26] that the unexpected large decay rates of Cabibbo-suppressed decay $D^+ \rightarrow \pi^+\pi^0$ and doubly-suppressed decay $D^0 \rightarrow K^+\pi^-$ observed experimentally imply a sizeable SU(3)-breaking effect. This effect can be explained in the factorization approach only if $f_+^{D\pi}(0) > f_+^{DK}(0)$ or $R > 1$. We find that explanation of the observed ratio R remains an unsolved issue in the light-front quark model.

Not shown in Fig. 5 is the heavy-to-light form factor $f_-(q^2)$, which is expected to satisfy the heavy-quark-symmetry relation at q^2 near zero recoil [22]: $(f_+ + f_-)^{B\pi} \sim 1/\sqrt{m_B}$ and $(f_+ + f_-)^{D\pi} \sim 1/\sqrt{m_D}$. Our light-front calculation shows that in general $f_-(q^2) \sim -f_+(q^2)$ is a good approximation for $B(D) \rightarrow \pi$ transitions even when q^2 is not close to q_{max}^2 , but it is only a rough approximation for $B(D) \rightarrow K$ transitions.

C. $P \rightarrow V$ Form Factors

The q^2 dependence of the form factors $V(q^2)$, $A_{0,1,2}(q^2)$ for $B \rightarrow D^*$ transition is depicted in Fig. 6. We see that the valence-quark contribution to V , A_0 and A_1 depends on the choice of the “+” or “−” reference frame, corresponding to $r(q^2) = r_+(q^2)$ or $r(q^2) = r_-(q^2)$. In general, the form factor in the “+” frame is larger than that in the “−” frame, but they become identical at zero recoil where $r_+(q_{\text{max}}^2) = r_-(q_{\text{max}}^2) = M_{D^*}/M_B$ [see (2.31-2.33)]. At maximum recoil $q^2 = 0$, we find

$$V^{BD^*}(0) = 0.78, \quad A_0^{BD^*}(0) = 0.73, \quad A_1^{BD^*}(0) = 0.68, \quad A_2^{BD^*}(0) = 0.61, \quad (4.7)$$

in the “+” frame where $r(0) = r_+(0) = 1$, and

$$V^{BD^*}(0) = 0.62, \quad A_0^{BD^*}(0) = 0.58, \quad A_1^{BD^*}(0) = 0.59, \quad A_2^{BD^*}(0) = 0.61, \quad (4.8)$$

which allows one to perform an analytic continuation to time-like momentum transfer. The Landau singularity there corresponds to our valence-quark contribution, while the non-Landau singularity to the non-valence configuration. However, the contribution of the Landau singularity in this approach vanishes at the “quark zero recoil” point (see Fig. 14 of [11] for $D \rightarrow K$ transition), a phenomenon not seen in our direct light-front calculations.

in the “−” frame where $r(0) = r_-(0) = (M_{D^*}/M_B)^2$ [see (2.33)]. As discussed in Sec. II.D, no firm predictions for V , A_0 , A_1 can be made unless the Z -graph contributions are included so that they are independent of the “±” frames. Although we do not have a reliable estimate for the Z -graph contribution, we know that it is more important for the $r = r_-$ curve than the $r = r_+$ one. This is because form factors at $q^2 = 0$ do not receive the non-valence contribution in the “+” frame because $r_+(0) = 1$. Therefore, (4.7) gives the complete results for $B \rightarrow D^*$ form factors at $q^2 = 0$. Consequently, the difference between (4.7) and (4.8) must be equal to the non-valence contribution in the “−” frame, namely,

$$\tilde{V}^{BD^*}(0) = 0.16, \quad \tilde{A}_0^{BD^*}(0) = 0.15, \quad \tilde{A}_1^{BD^*}(0) = 0.08, \quad \tilde{A}_2^{BD^*}(0) = 0. \quad (4.9)$$

This implies that *for heavy-to-heavy transition, form factors calculated from the valence-quark configuration alone and evaluated in the “+” frame should be reliable in a broad kinematic region and become most trustworthy in the close vicinity of maximum recoil*. A generic feature of the Z -graph effect is illustrated in Fig. 7 by considering the form factor $A_0^{BD^*}$. Assuming that the full $A_0^{BD^*}$ has a dipole behavior shown in Fig. 7 with a pole mass $M_{\text{pole}} = 6.73$ GeV (dash-dotted curve), the difference between the “full curve” and the valence contribution should give the non-valence contribution. It is clear that the Z -graph effect in the “−” frame (dashed curve) is sizeable in the entire kinematic region, whereas it is important in the “+” frame (solid curve) only when q^2 is close to the zero-recoil point.

For a broad range of q^2 , we find that $A_0^{BD^*}$, $A_2^{BD^*}$, V^{BD^*} can be fitted to a dipole form and $A_1^{BD^*}$ to a monopole form, in accord with the HQS relations given in (3.24). Experimentally, two form-factor ratios defined by

$$\begin{aligned} R_1(q^2) &= \left[1 - \frac{q^2}{(M_B + M_{D^*})^2} \right] \frac{V^{BD^*}(q^2)}{A_1^{BD^*}(q^2)}, \\ R_2(q^2) &= \left[1 - \frac{q^2}{(M_B + M_{D^*})^2} \right] \frac{A_2^{BD^*}(q^2)}{A_1^{BD^*}(q^2)}, \end{aligned} \quad (4.10)$$

have been extracted by CLEO [27] from an analysis of angular distribution in $\bar{B} \rightarrow D^* \ell \bar{\nu}$ decays with the results:

$$R_1(q_{\text{max}}^2) = 1.18 \pm 0.30 \pm 0.12, \quad R_2(q_{\text{max}}^2) = 0.71 \pm 0.22 \pm 0.07. \quad (4.11)$$

(3.24) implies that, irrespective of the values of q^2 , $R_1(q^2) = R_2(q^2) = 1$ in the heavy-quark limit. Our light-front calculations yield $V^{BD^*}(q_{\text{max}}^2) = 1.14$, $A_1^{BD^*}(q_{\text{max}}^2) = 0.83$,

and $A_2^{BD^*}(q_{\max}^2) = 0.96$, hence $R_1(q_{\max}^2) = 1.11$ and $R_2(q_{\max}^2) = 0.92$, in agreement with experiment. The predictions of HQET are similar [2]: $R_1 \simeq 1.3 \pm 0.1$ and $R_2 \simeq 0.8 \pm 0.2$.

As shown in Figs. 8-11, we have also computed the q^2 dependence of the form factors for $B \rightarrow K^*$, $B \rightarrow \rho$, $D \rightarrow K^*$ and $D \rightarrow \rho$ decays. The numerical results of the form factors at $q^2 = 0$ are (in the “+” frame):

$$\begin{aligned}
B \rightarrow K^* : \quad & A_0^{BK^*}(0) = 0.32, \quad A_1^{BK^*}(0) = 0.26, \quad A_2^{BK^*}(0) = 0.23, \quad V^{BK^*}(0) = 0.35, \\
D \rightarrow K^* : \quad & A_0^{DK^*}(0) = 0.71, \quad A_1^{DK^*}(0) = 0.62, \quad A_2^{DK^*}(0) = 0.46, \quad V^{DK^*}(0) = 0.87, \\
B \rightarrow \rho : \quad & A_0^{B\rho}(0) = 0.28, \quad A_1^{B\rho}(0) = 0.20, \quad A_2^{B\rho}(0) = 0.18, \quad V^{B\rho}(0) = 0.30, \\
D \rightarrow \rho : \quad & A_0^{D\rho}(0) = 0.63, \quad A_1^{D\rho}(0) = 0.51, \quad A_2^{D\rho}(0) = 0.34, \quad V^{D\rho}(0) = 0.78.
\end{aligned} \tag{4.12}$$

Experimentally, only $D \rightarrow K^*$ form factors have been measured with the results [23]

$$V^{DK^*}(0) = 1.1 \pm 0.2, \quad A_1^{DK^*}(0) = 0.56 \pm 0.04, \quad A_2^{DK^*}(0) = 0.40 \pm 0.08, \tag{4.13}$$

obtained by assuming a pole behavior for the q^2 dependence. Our predictions for the $D \rightarrow K^*$ form factors are consistent with experiment.

Table II. Form factors for $B \rightarrow \rho$ and $D \rightarrow \rho$ transitions at $q^2 = 0$ in various models.

	Reference	$A_1^{B\rho}(0)$	$A_2^{B\rho}(0)$	$V^{B\rho}(0)$	$A_1^{D\rho}(0)$	$A_2^{D\rho}(0)$	$V^{D\rho}(0)$
Lattice	BES [28]	—	—	—	0.65^{+15+24}_{-15-23}	0.59^{+31+28}_{-31-25}	$1.07 \pm 0.49 \pm 0.35$
	LMMS [29]	—	—	—	0.45 ± 0.04	0.02 ± 0.26	0.78 ± 0.12
	ELC [30]	0.22 ± 0.05	$0.49 \pm 0.21 \pm 0.05$	0.37 ± 0.11	—	—	—
	APE [31]	0.24 ± 0.12	0.27 ± 0.80	0.53 ± 0.31	—	—	—
	UKQCD [32]	0.27^{+7+3}_{-4-3}	0.28^{+9+4}_{-6-5}	—	—	—	—
	GSS [33]	0.16^{+4+22}_{-4-16}	0.72^{+35+10}_{-35-7}	0.61^{+23+9}_{-23-6}	0.59^{+7+8}_{-7-6}	0.83^{+20+12}_{-20-8}	1.31^{+25+18}_{-25-13}
Sum Rule	S [34]	0.96 ± 0.15	1.21 ± 0.18	1.27 ± 0.12	—	—	—
	Ball [35]	0.5 ± 0.1	0.4 ± 0.2	0.6 ± 0.2	0.5 ± 0.2	0.4 ± 0.1	1.0 ± 0.2
	ABS [36]	0.24 ± 0.04	—	0.28 ± 0.06	—	—	—
	Narison [37]	0.38 ± 0.04	0.45 ± 0.05	0.45 ± 0.05	—	—	—
	YH [38]	0.07 ± 0.01	0.16 ± 0.01	0.19 ± 0.01	0.34 ± 0.08	0.57 ± 0.08	0.98 ± 0.11
QM	ISGW [39]	0.05	0.02	0.27	—	—	—
	BSW [18]	0.28	0.28	0.33	0.78	0.92	1.23
	Stech [40]	0.32	0.35	0.37	—	—	—
	FGM [41]	0.26 ± 0.03	0.31 ± 0.03	0.29 ± 0.03	—	—	—
	IV [42]	0.50	0.51	0.70	0.55	0.45	1.08
LFQM	this work	0.20	0.18	0.30	0.51	0.34	0.78
	OXT [9]	0.21	0.18	0.32	—	—	—
	Jaus [10]	0.26	0.24	0.35	0.58	0.42	0.93
	Melikhov [11]	0.17-0.26	0.16-0.24	0.22-0.34	—	—	—
HQET +ChPT	CDDGFN [43]	0.21	0.20	1.04	0.55	0.28	1.01
	CDDGFN [44]	0.28	0.19	0.50	—	—	—

Form factors for $B \rightarrow \rho$ and $D \rightarrow \rho$ transitions at $q^2 = 0$ predicted in various approaches (lattice simulations, QCD sum rule, quark model, light-front quark model, and heavy quark effective theory together with chiral perturbation theory) are summarized in Table II. We have to await further experimental studies in order to test various models. The $B \rightarrow K$ and $B \rightarrow K^*$ transitions arise from flavor-changing neutral currents induced by QCD corrections. It has been found recently that there are two experimental data for $B \rightarrow J/\psi K^{(*)}$ which cannot be accounted for simultaneously by all commonly used models [45]. Hence, it is important to have a reliable estimate of the $B \rightarrow K^{(*)}$ form factors at $q^2 = m_{J/\psi}^2$ in order to test the validity of the factorization approach. Our calculation gives

$$\begin{aligned}
F_1^{BK^*}(m_{J/\psi}^2) &= 0.66, & V_2^{BK^*}(m_{J/\psi}^2) &= 0.42, \\
A_0^{BK^*}(m_{J/\psi}^2) &= 0.63, & A_1^{BK^*}(m_{J/\psi}^2) &= 0.37, & A_2^{BK^*}(m_{J/\psi}^2) &= 0.43,
\end{aligned} \tag{4.14}$$

from valence-quark configuration.

As for the q^2 dependence of heavy-to-light form factors, we see from Figs. 8-11 that, except for $V^{B\rho}$, they all increase with q^2 , though A_1 is flatter than A_0 , A_2 , and V . As we have argued before, the valence-quark contribution evaluated in the “+” frame should be reliable when q^2 is close to maximum recoil. For small q^2 , we have a dipole behavior for A_0 , A_2 , V (except for $V^{B\rho}$ and V^{BK^*}) and a monopole behavior for A_1 ; that is, A_0 , A_2 , and V increase with q^2 faster than A_1 . The form factor V for $B \rightarrow \rho$ and $B \rightarrow K^*$ in the “+” frame do not have a dipole behavior at small q^2 mainly because of the large destructure contributions from the $\Theta_V k_\perp^2/W_V$ terms in (2.78). As a result, the form factor V in $B \rightarrow \rho$ and $B \rightarrow K^*$ decays evaluated in the “+” frame is smaller than that in the “-” frame. The q^2 dependence of the $P \rightarrow V$ form factors have also been studied in the QCD-sum-rule approach with some contradicting results. For example, while $A_1^{B\rho}$ is found to decrease from $q^2 = 0$ to $q^2 = 15 \text{ GeV}^2$ in [46] (see also [35,37,42]), such a phenomenon is not seen in [36,38] (see also Sec. 5.3 of [44]). The sum-rule results of [38] show that the form factors A_0 , A_2 , V all have a dipole form while A_1 has a monopole form, in accord with our observation. The same conclusion is also reached in [9] based on the scaling behavior of heavy-to-light form factors in the $m_Q \rightarrow \infty$ limit. A recent lattice study of the axial form factors $A_0^{B\rho}$, $A_1^{B\rho}$ and $A_3^{B\rho}$ [32] is consistent with the q^2 behavior we have in the light-front quark model.

V. SUMMARY

The heavy-to-heavy and heavy-to-light form factors in $P \rightarrow P$ and $P \rightarrow V$ transitions are studied in the present paper. In the light-front relativistic quark model, the decay form factors are evaluated in a frame where $q^+ \geq 0$ and $q_\perp = 0$, so that it covers the entire physical range of momentum transfer and no extrapolation assumption from $q^2 = 0$ or from $q^2 = q_{\text{max}}^2$ is required. In previous works using $q^+ = 0$, one can only calculate form factors at $q^2 = 0$; moreover, the form factors $f_-(q^2)$ in $P \rightarrow P$ decay and $a_-(q^2)$ in $P \rightarrow V$ decay cannot be studied. For the first time, we have calculated the $P \rightarrow V$ form factors directly at time-like momentum transfers. The main results of this paper are :

- 1). We have investigated the behavior of heavy-to-heavy form factors in the heavy-quark limit and found that the requirements of heavy-quark symmetry (2.29) for $P \rightarrow P$ transition and (2.51) for $P \rightarrow V$ transition are indeed fulfilled by the light-front quark model provided that the universal function $\zeta(v \cdot v')$ obtained from $P \rightarrow V$ decay is identical to the Isgur-Wise

function $\xi(v \cdot v')$ in $P \rightarrow P$ decay.

2). Contrary to the Isgur-Wise function in $P \rightarrow P$ decay, the normalization of $\zeta(v \cdot v')$ at zero recoil depends on the light-front wave function used. We found that the BSW amplitude correctly gives $\xi(1) = 1$, but $\zeta(1) = 0.87$. Therefore, this type of wave functions cannot describe $P \rightarrow V$ decays in a manner consistent with heavy-quark symmetry.

3). Using the Gaussian-type amplitude, the Isgur-Wise function $\zeta(v \cdot v')$ has a correct normalization at zero recoil and is identical to $\xi(v \cdot v')$ numerically up to six digits. It can be fitted very well with a dipole dependence with $M_{\text{pole}} = 6.65$ GeV for $B \rightarrow D$ transition. However, the predicted slope parameter $\rho^2 = 1.24$ is probably too large. This may be ascribed to the fact that the Gaussian-type wave function does not have enough high-momentum components at large k_{\perp} .

4). The valence-quark and non-valence contributions to form factors are in general dependent on the recoiling direction of the daughter meson relative to the parent meson, but their sum should not. Although we do not have a reliable estimate of the pair-creation effect, we have argued that, for heavy-to-heavy transition, form factors calculated from the valence-quark configuration evaluated in the “+” frame should be reliable in a broad kinematic region, and they become most trustworthy in the vicinity of maximum recoil.

5). The form factors F_1 , A_0 , A_2 , V (except for $V^{B\rho}$ and V^{BK^*}) all exhibit a dipole behavior, which F_0 and A_1 show a monopole behavior in the close vicinity of maximum recoil for heavy-to-light transition, and in a broader kinematic region for heavy-to-heavy decays. Therefore, F_1 , A_0 , A_2 , V increase with q^2 faster than F_0 and A_1 .

ACKNOWLEDGMENTS

This work was supported in part by the National Science Council of ROC under Contract Nos. NSC85-2112-M-001-010 and NSC85-2112-M-001-023.

REFERENCES

- [1] N. Isgur and M.B. Wise, *Phys. Lett.* **B232**, 113 (1989); **B237**, 527 (1990).
- [2] M. Neubert, *Phys. Rep.* **245**, 261 (1994).
- [3] M.V. Terent'ev, *Sov. J. Phys.* **24**, 106 (1976); V.B. Berestetsky and M.V. Terent'ev, *ibid.* **24**, 547 (1976); **25**, 347 (1977).
- [4] P.L. Chung, F. Coester, and W.N. Polyzou, *Phys. Lett.* **B205**, 545 (1988).
- [5] W. M. Zhang, *Chin. J. Phys.* **31**, 717 (1994); Preprint IP-ASTP-19-95 [hep-ph/9510428].
- [6] W. Jaus, *Phys. Rev.* **D41**, 3394 (1990); *ibid.* **D44**, 2851 (1991); *Z. Phys.* **C54**, 611 (1992).
- [7] P.J. O'Donnell and Q.P. Xu, *Phys. Lett.* **B325**, 219 (1994).
- [8] P.J. O'Donnell and Q.P. Xu, *Phys. Lett.* **B336**, 113 (1994).
- [9] P.J. O'Donnell, Q.P. Xu, and H.K.K. Tung, *Phys. Rev.* **D52**, 3966 (1995).
- [10] W. Jaus, *Phys. Rev.* **D53**, 1349 (1996).
- [11] D. Melikhov, *Phys. Rev.* **D53**, 2460 (1996); hep-ph/9603340; hep-ph/9607216 (1996).
- [12] C.Y. Cheung, C.W. Hwang, and W.M. Zhang, hep-ph/9602309 (1996).
- [13] N.B. Demchuk, I.L. Grach, I.M. Narodetskii, and S. Simula, INFN-ISS 95/18 [hep-ph/9601369].
- [14] I.L. Grach, I.M. Narodetskii, and S. Simula, INFN-ISS 96/4 [hep-ph/9605349].
- [15] A. Dubin and A. Kaidalov, *Yad. Fiz.* **56**, 164 (1993) [*Phys. At. Nucl.* **56**, 237 (1993)].
- [16] M. Sawicki, *Phys. Rev.* **D44**, 433 (1991).
- [17] C.Y. Cheung, W.M. Zhang, and G.L. Lin, *Phys. Rev.* **D52**, 2915 (1995).
- [18] M. Wirbel, B. Stech, and M. Bauer, *Z. Phys.* **C29**, 637 (1985); M. Bauer, B. Stech, and M. Wirbel, *ibid.* **42**, 671 (1989).
- [19] S. Simula, *Phys. Lett.* **B373**, 193 (1996).
- [20] M. Neubert and V. Rieckert, *Nucl. Phys.* **B382**, 97 (1992).
- [21] M. Neubert, CERN-TH/96-55 [hep-ph/9604412].
- [22] N. Isgur and M. B. Wise, *Phys. Rev.* **D41**, 151 (1990).
- [23] Particle Data Group, *Phys. Rev.* **D50**, 1173 (1994).
- [24] CLEO Collaboration, M.S. Alam *et al.*, *Phys. Rev. Lett.* **71**, 1311 (1993).
- [25] CLEO Collaboration, F. Butler *et al.*, *Phys. Rev.* **D52**, 2656 (1995).
- [26] L.L. Chau and H.Y. Cheng, *Phys. Lett.* **B333**, 514 (1994).

- [27] CLEO Collaboration, J.E. Duboscq *et al.*, *Phys. Rev. Lett.* **76**, 3898 (1996).
- [28] G. Bernard, A. El Khadra, and A. Soni, *Phys. Rev.* **D43**, 2140 (1992).
- [29] V. Lubicz, G. Martinelli, M.S. McCarthy, and C.T. Sachrajda, *Phys. Lett.* **B274**, 415 (1992).
- [30] A. Abada *et al.*, *Nucl. Phys.* **B416**, 675 (1994).
- [31] APE Collaboration, C.R. Allton *et al.*, *Phys. Lett.* **B345**, 513 (1995).
- [32] UKQCD Collaboration, D.R. Burford *et al.*, *Nucl. Phys.* **B447**, 425 (1995); J.M. Flynn *et al.*, *Nucl. Phys.* **B461**, 327 (1996); J.M. Flynn and J. Nieves, UG-DFM-3/96 [hep-ph/9602201].
- [33] S. Güsken, G. Siegert, and K. Schilling, *Nucl. Phys. B (Proc. Suppl.)* **47**, 485 (1996).
- [34] V.A. Slobodenyuk, *Sov. J. Nucl. Phys.* **51**, 696 (1990).
- [35] P. Ball, *Phys. Rev.* **D48**, 3190 (1993).
- [36] A. Ali, V.M. Braun, and H. Simma, *Z. Phys.* **C63**, 437 (1994).
- [37] S. Narison, *Phys. Lett.* **B345**, 166 (1995).
- [38] K.C. Yang and W-Y.P. Hwang, NUTHU-94-17, to appear in *Z. Phys.* (1996).
- [39] N. Isgur, D. Scora, B. Grinstein, and M.B. Wise, *Phys. Rev.* **D39**, 799 (1989).
- [40] B. Stech, *Phys. Lett.* **B354**, 447 (1995); HD-THEP-95-54 [hep-ph/9512414].
- [41] R.N. Faustov, V.O. Galkin, and A.Yu. Mishurov, *Phys. Rev.* **D53**, 6302 (1996); *Phys. Lett.* **B356**, 516 (1995).
- [42] M.A. Ivanov and Yu.M. Valit, hep-ph/9606404.
- [43] R. Casalbuoni, A. Deandrea, N. Di Bartolomeo, R. Gatto, F. Feruglio, and G. Nardulli, *Phys. Lett.* **B299**, 139 (1993).
- [44] R. Casalbuoni, A. Deandrea, N. Di Bartolomeo, R. Gatto, F. Feruglio, and G. Nardulli, UGVA-DPT 1996/05-928 [hep-ph/9605342].
- [45] M. Gourdin, A.N. Kamal, and X.Y. Pham, *Phys. Rev. Lett.* **73**, 3355 (1994); R. Aleksan, A. Le Yaouanc, L. Oliver, O. Pène, and J.-C. Raynal, *Phys. Rev.* **D51**, 6235 (1995).
- [46] P. Ball, V.M. Braun, and H.G. Dosh, *Phys. Rev.* **D44**, 3567 (1991).

FIGURE CAPTIONS

Fig. 1 The Feynman triangle diagram and the corresponding light-front subdiagrams. Diagram (a) corresponds to the valence-quark configuration and diagram (b) to the non-valence configuration.

Fig. 2 The Isgur-Wise function $\xi(v \cdot v')$ for $P \rightarrow P$ transition calculated using Gaussian-type (solid line) and BSW-type (dashed line) light-front wave functions. For comparison, a curve for $1/v \cdot v'$ is also shown.

Fig. 3 The Isgur-Wise function $\zeta(v \cdot v')$ for $P \rightarrow V$ transition calculated using Gaussian-type (solid line) and BSW-type (dashed line) light-front wave functions.

Fig. 4 Form factors $F_1(q^2) = f_+(q^2)$ and $F_0(q^2)$ for $B \rightarrow D$ transition arising from the valence-quark configuration. Dashed curves are fits to F_1 in a dipole form with $M_{\text{pole}} = 6.59$ GeV and to F_0 in a monopole form with $M_{\text{pole}} = 7.90$ GeV.

Fig. 5 The form factor $f_+(q^2)$ for $B \rightarrow \pi$, $B \rightarrow K$, $D \rightarrow \pi$ and $D \rightarrow K$ transitions arising from the valence-quark configuration.

Fig. 6 Form factors $V(q^2)$, $A_0(q^2)$, $A_1(q^2)$ and $A_2(q^2)$ for $B \rightarrow D^*$ transition. Solid lines are the valence contribution evaluated in the “+” frame where $r(q^2) = r_+(q^2)$, and dashed lines in the “−” frame where $r(q^2) = r_-(q^2)$. The contribution to the form factor A_2 is independent of the choice of the “+” or “−” frame.

Fig. 7 An illustration of the non-valence contribution to the form factor $A_0^{BD^*}$, whose general feature applies to $A_1^{BD^*}$ and $V_0^{BD^*}$ as well. Valence-quark contributions to $A_0^{BD^*}$ evaluated in the “+” frame (solid line) and in the “−” frame (dashed line) are the same as in Fig.6. The corresponding non-valence contribution are extracted in respective frames by assuming that the full $A_0^{BD^*}$ has a dipole behavior with $M_{\text{pole}} = 6.73$ GeV (dash-dotted line).

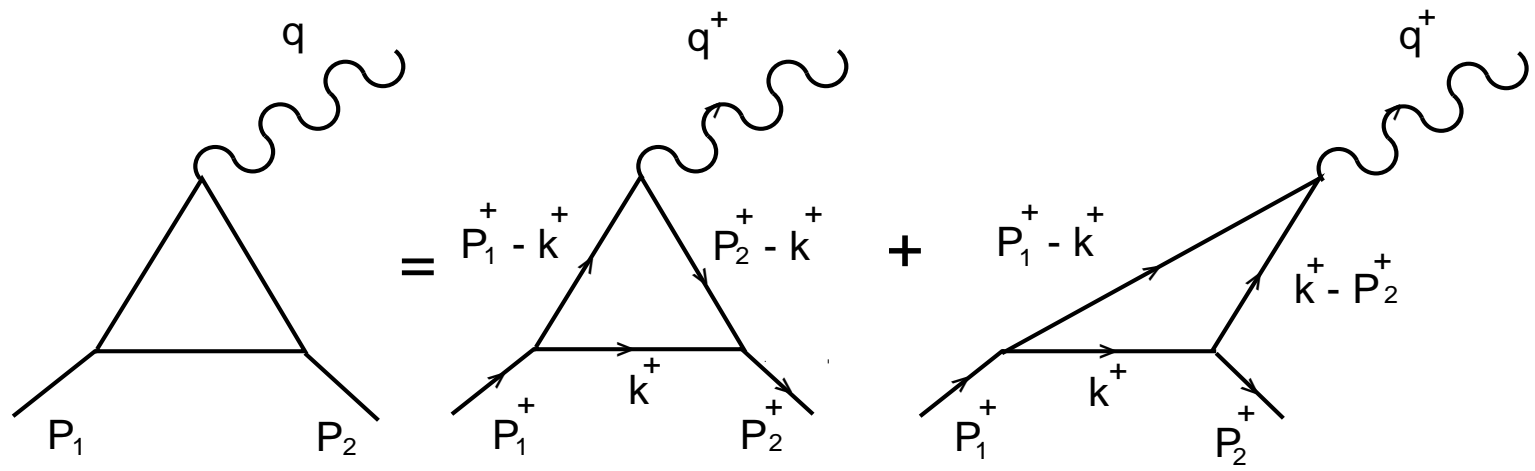
Fig. 8 Same as Fig. 6 except for $B \rightarrow K^*$ transition.

Fig. 9 Same as Fig. 6 except for $B \rightarrow \rho$ transition.

Fig. 10 Same as Fig. 6 except for $D \rightarrow K^*$ transition.

Fig. 11 Same as Fig. 6 except for $D \rightarrow \rho$ transition.

Fig.1



FIGURES

Fig.2

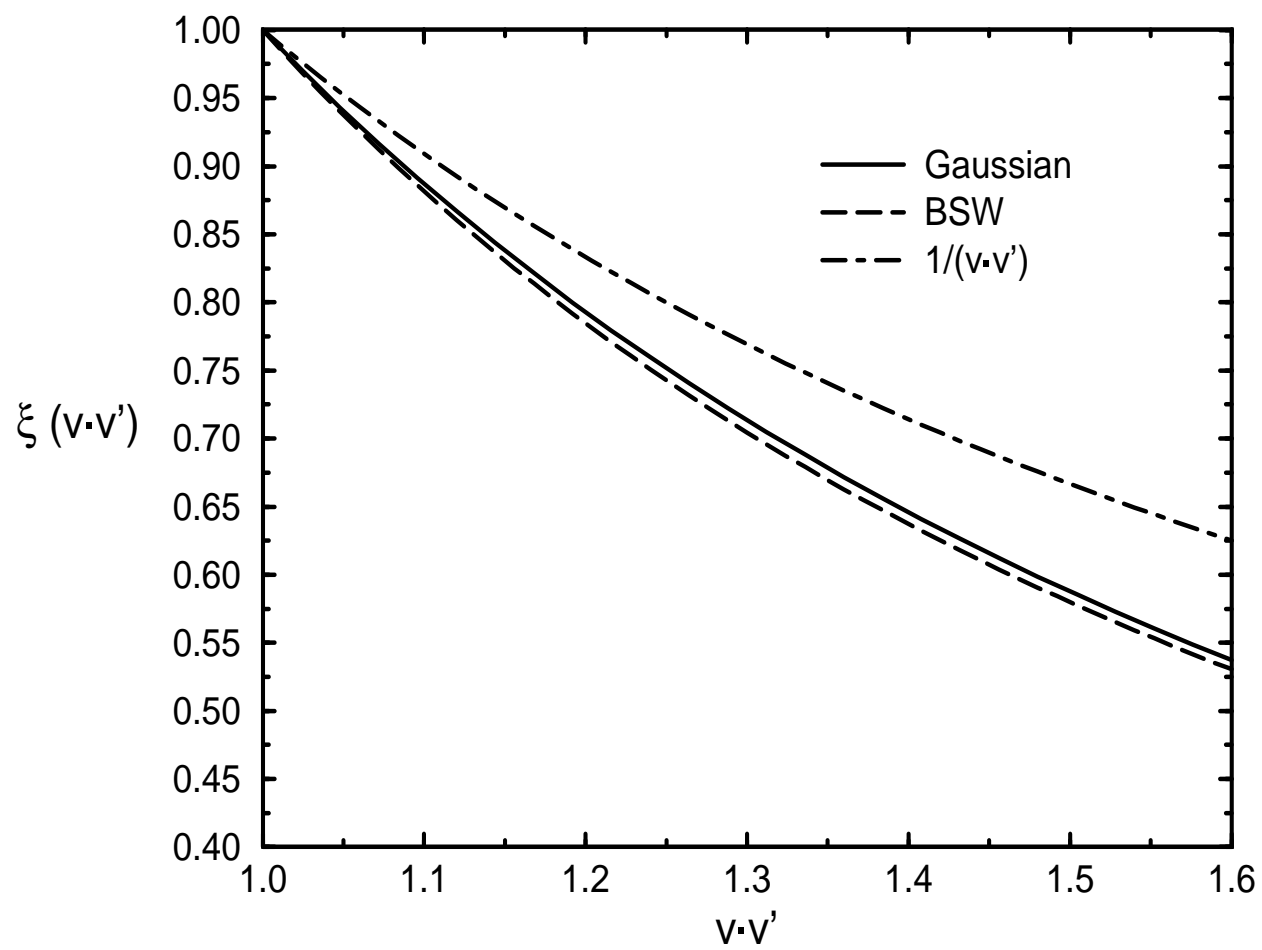


Fig.3

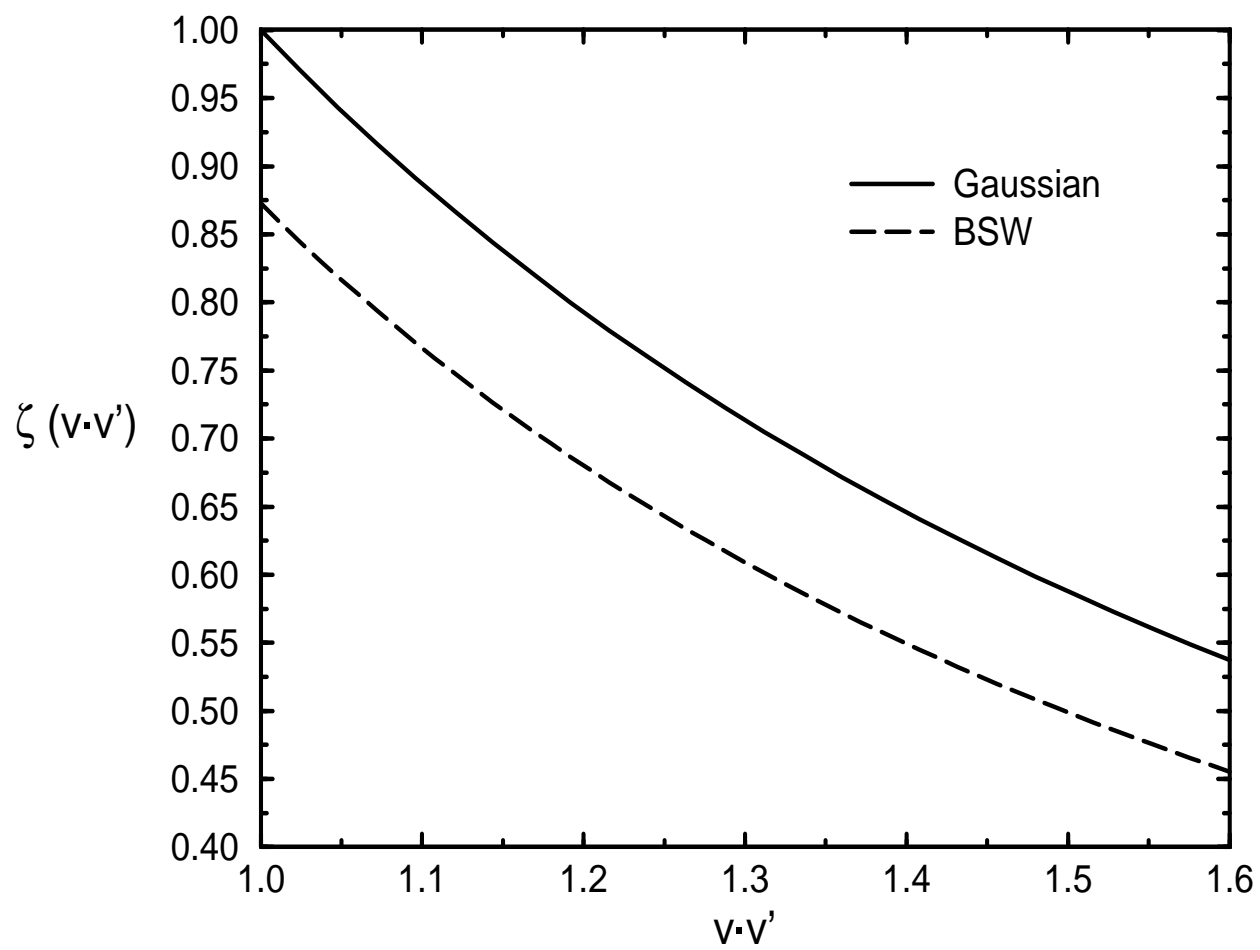


Fig.4

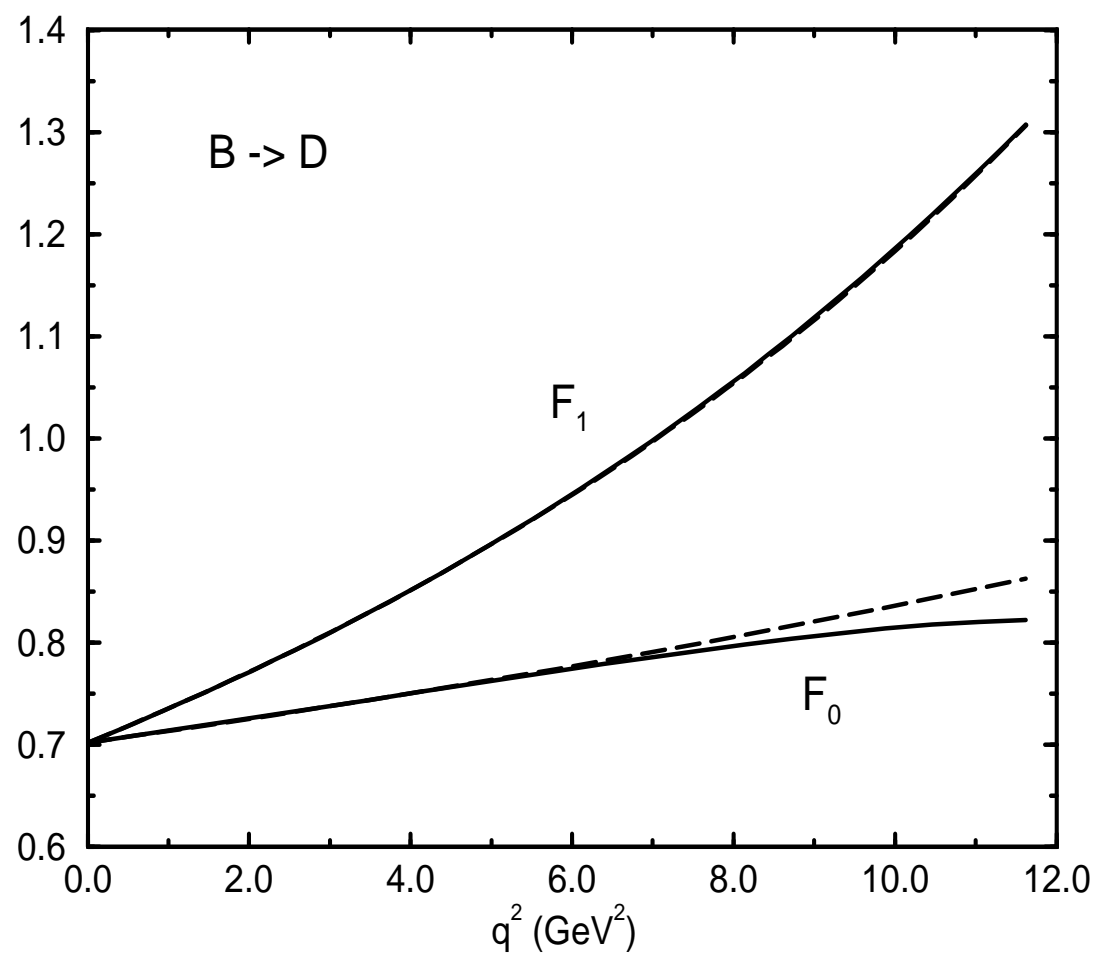


Fig.5

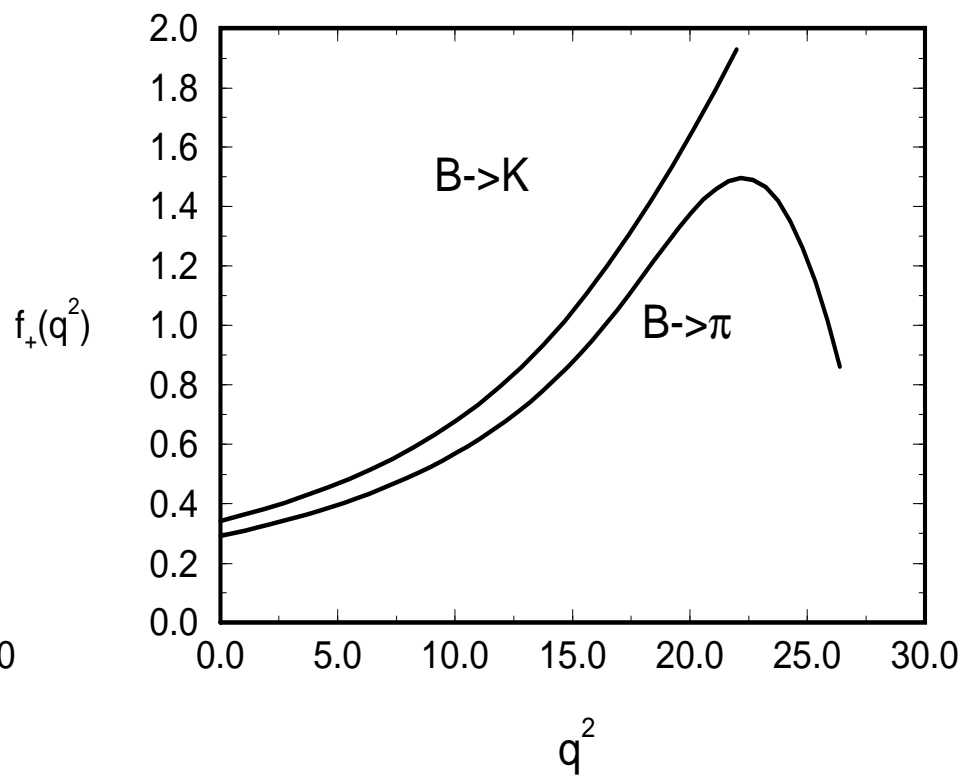
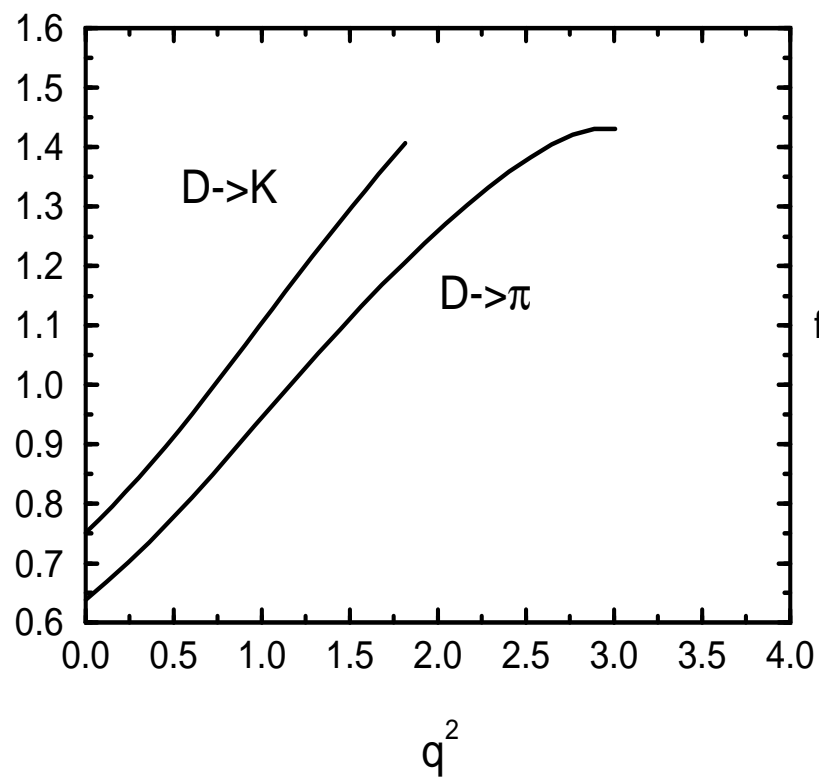


Fig.6

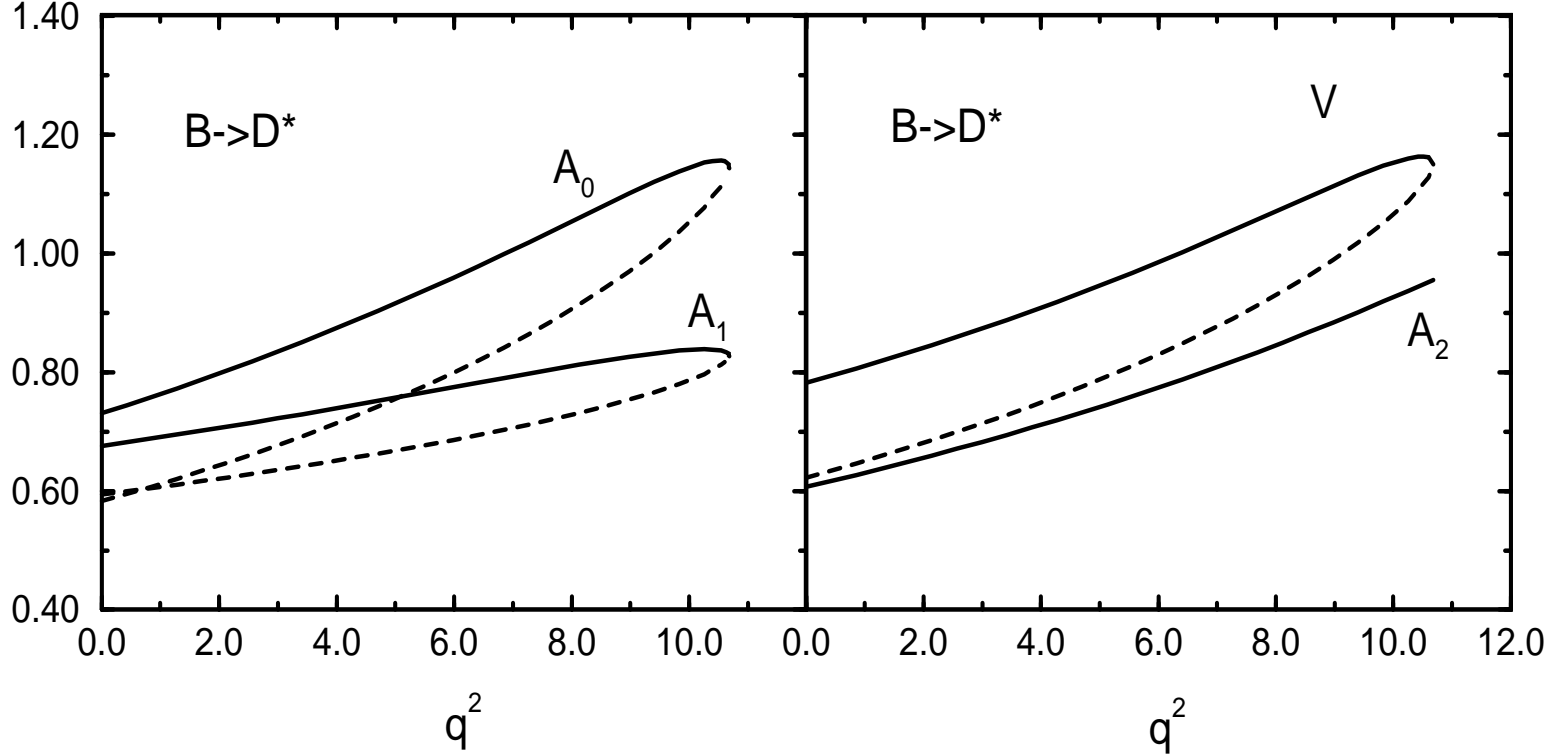


Fig.7

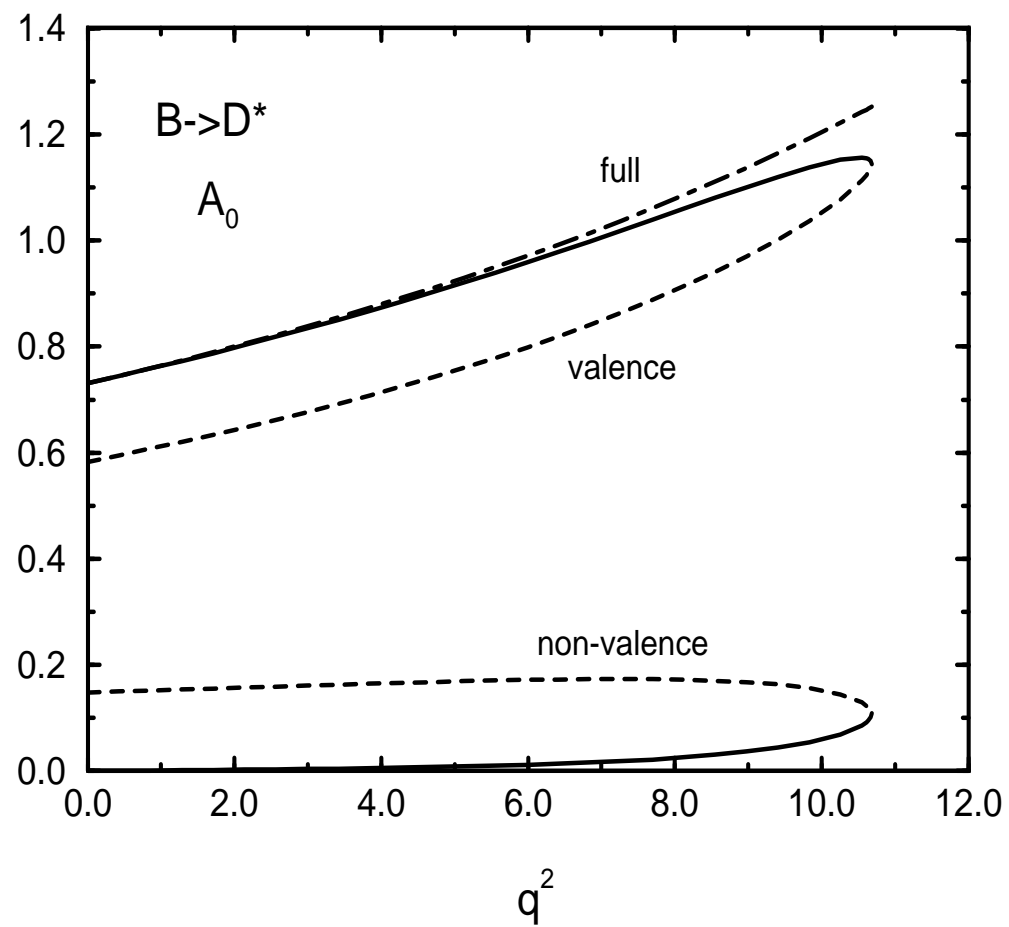


Fig.8

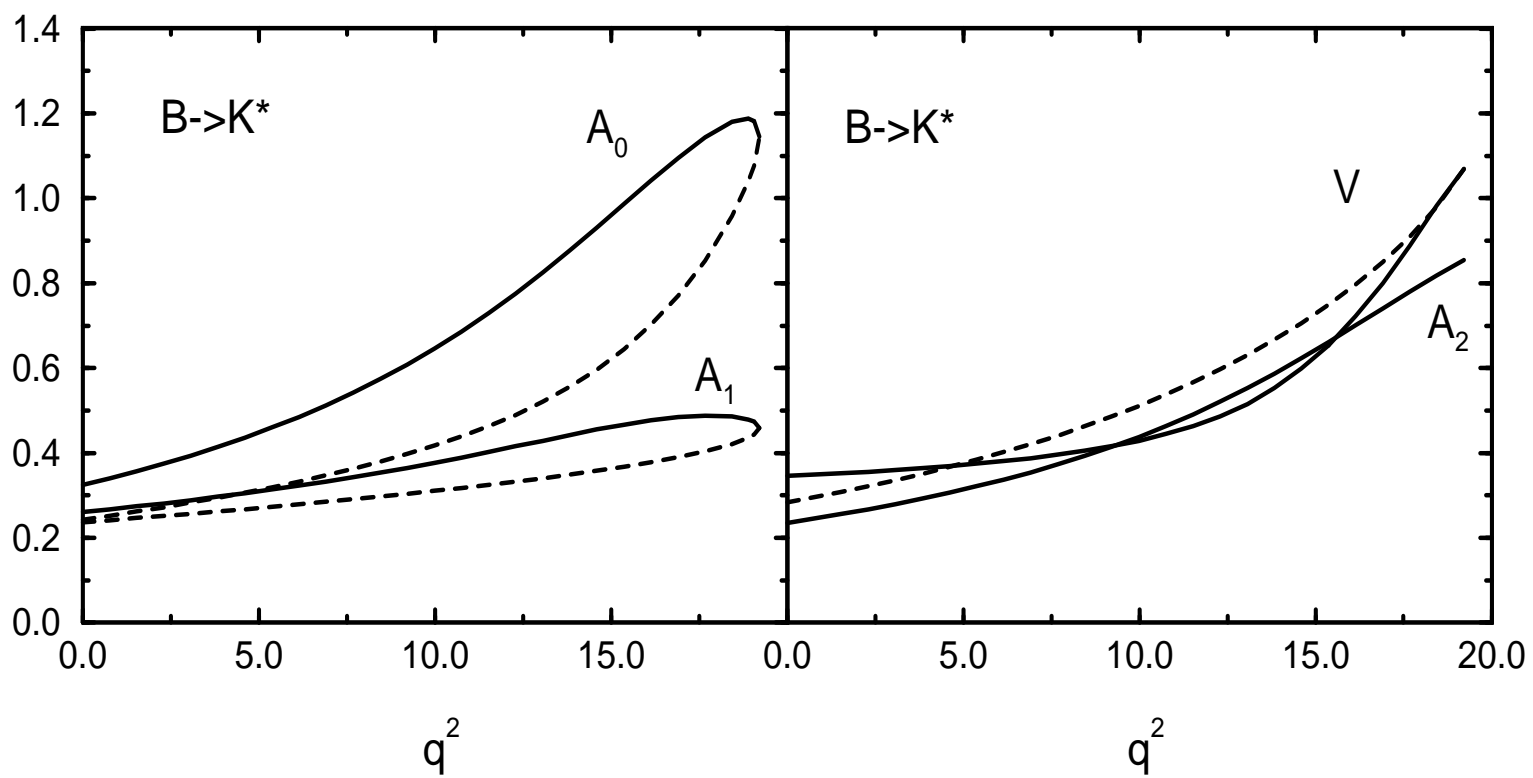


Fig.9

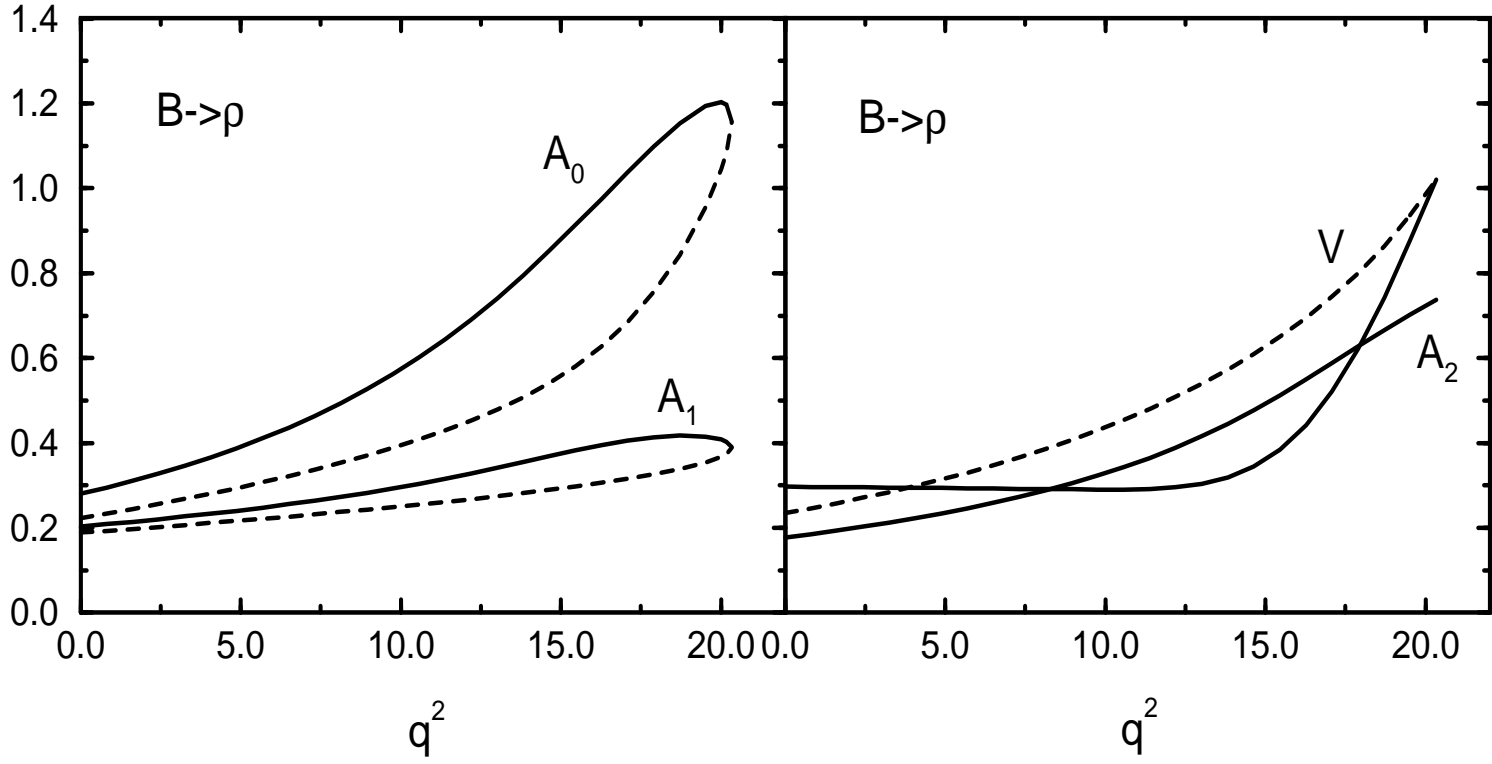


Fig.10

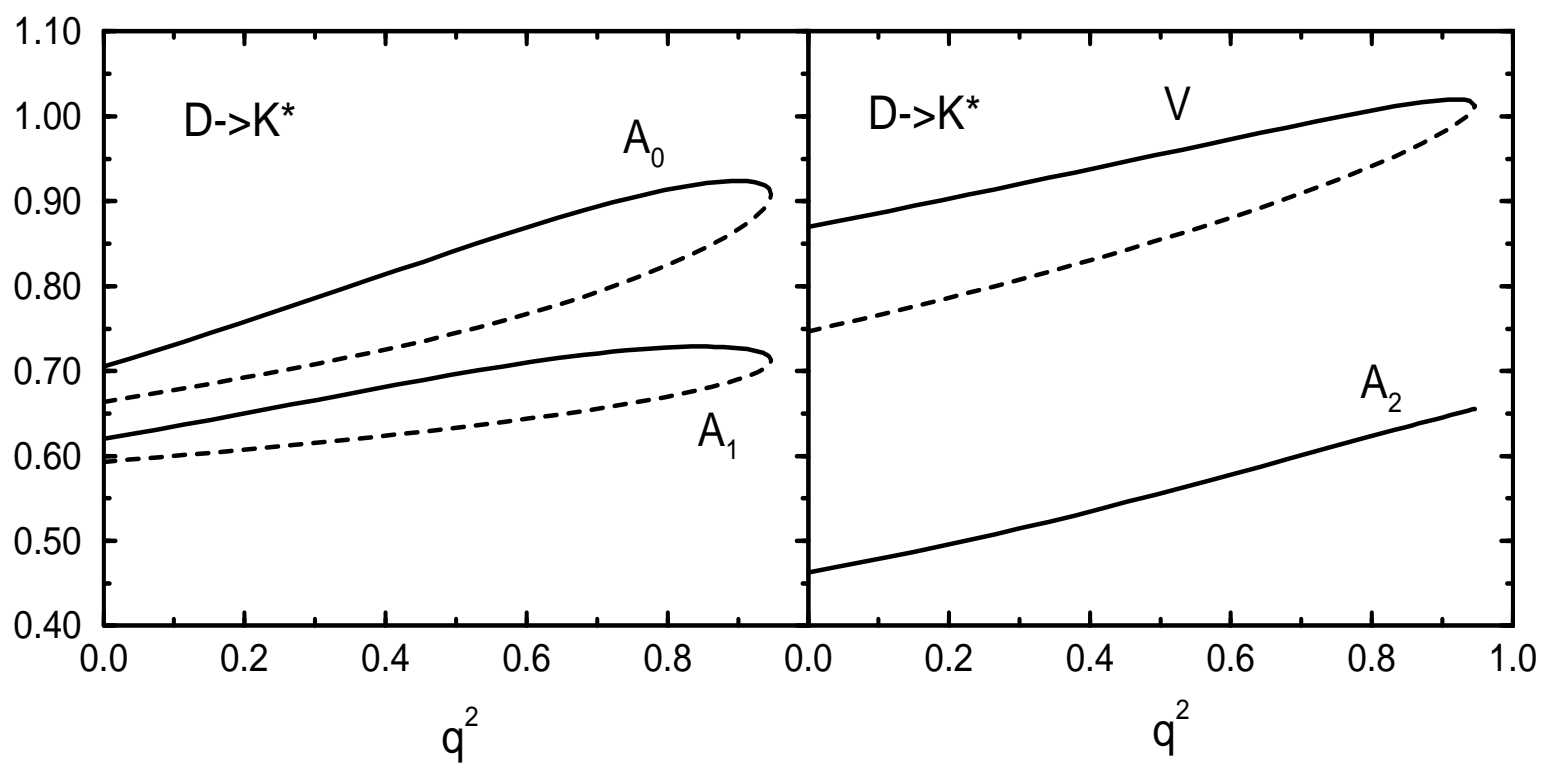


Fig.11

